DRL NO. 74/DRD NO. SE
Line Item No. 7

DOE/JPL-955089 - 81/12
Distribution Category UC-63

SILICON SOLAR CELL PROCESS DEVELOPMENT, FABRICATION AND ANALYSIS

ANNUAL REPORT (PHASE III)

For Period Covering
1 July 1980 to 31 June 1981

By:

H.I. Yoo, P.A. Iles, and D.C. Leung

JPL Contract No. 955089

OPTICAL COATING LABORATORY, INC.
Photoelectronics Division
15251 E. Don Julian Road
City of Industry, California 91746

"The JPL Low-Cost Silicon Solar Array Project is sponsored by the U.S. Department of Energy and forms part of the Solar Photovoltaic Conversion Program to initiate a major effect toward the development of low-cost solar arrays. This work was performed for the Jet Propulsion Laboratory, California Institute of Technology by agreement between NASA and DOE."

DRL NO. 74/DRD NO. SE
Line Item No. 7

DOE/JPL-955089 - 81/12
Distribution Category UC-63

SILICON SOLAR CELL PROCESS

DEVELOPMENT, FABRICATION AND ANALYSIS

ANNUAL REPORT (PHASE III)

For Period Covering
1 July 1980 to 31 June 1981

By:

H.I. Yoo, P.A. Iles, and D.C. Leung

JPL Contract No. 955089

OPTICAL COATING LABORATORY, INC.
Photoelectronics Division
15251 E. Don Julian Road
City of Industry, California 91746

"The JPL Low-Cost Silicon Solar Array Project is sponsored by the U.S. Department of Energy and forms part of the Solar Photovoltaic Conversion Program to initiate a major effect toward the development of low-cost solar arrays. This work was performed for the Jet Propulsion Laboratory, California Institute of Technology by agreement between NASA and DOE."

ABSTRACT

Solar cells were fabricated from EFG ribbons (Mobil-Tyco), Dendritic webs (Westinghouse), Cast Ingots by Heat Exchanger Method (HEM, Crystal Systems), and Cast Ingots by Ubiquitous Crystallization Process (UCP, Semix). Baseline and other process variations were applied to fabricate solar cells.

EFG ribbons grown in a carbon-containing gas atmosphere showed significant improvement in silicon quality. This new EFG demonstrated an average baseline efficiency of 10.3% as opposed to 8.0% AM1 for the earlier EFG. The best efficiency achieved by the advanced process was 13.8% under AM1 conditions.

Baseline solar cells from dendritic webs of various runs indicated that the quality of the webs under investigation was not as good as the conventional CZ silicon, showing an average minority carrier diffusion length of about 60um versus 120um of CZ wafers.

Detail evaluation of large cast ingots by HEM showed ingot reproducibility problems from run to run and uniformity problems of sheet quality within an ingot. Junction shunting was a major problem area, probably caused by the particulate inclusions observed in the bulk.

Initial evaluation of the wafers prepared from the cast polycrystalline ingots by UCP suggested that the quality of the wafers from this process is considerably lower than the conventional CZ wafers. Overall performance was relatively uniform, except for a few cells which showed shunting problems caused by inclusions.

TABLE OF CONTENTS

LIST OF FIGURES

LIST OF TABLES

I. INTRODUCTION

The objective of this program is to investigate, develop, and utilize technologies appropriate and necessary for improving the efficiency of solar cells made from various unconventional silicon sheets. During the third phase of the program, work has progressed in fabrication and characterization of solar cells from EFG ribbons (Mobil-Tyco), cast ingots by Heat Exchanger Method (HEM, Crystal Systems), and cast ingots by Ubiguitous Crystallization Process (UCP, Semix). Solar cells were fabricated using a baseline process typical of those used currently in the silicon solar cell industry. Other process modifications were included to give indications of the possible improved performance obtainable from various sheets. Process variations used included gettering by diffusion glasses, low temperature annealing, shallow junction formation, application of fine front grid lines, formation of back surface field (BSF) and back surface reflector (BSR), and application of better AR coating (i.e., multi-layer anti-reflective coating).

The solar cell parameters measured included open circuit voltage (Voc), short circuit current density (Jsc), curve fill factor (CFF) and conversion efficiency n (all taken under AM1 illumination). Also, measurements for typical cells included spectral response, dark I-V characteristics, minority carrier diffusion length, and photoresponse by fine light spot scanning.

The results were compared to the properties of cells made from conventional single crystalline Czochralski silicon with an emphasis on statistical evaluation. Limited efforts were also made to identify impurity levels in certain portions of HEM ingots using Deep Level Transient Spectroscopy (DLTS).

II. TECHNICAL DISCUSSION*

A. EFG Solar Cells

1.0 Solar Cell Fabrication

EFG Ribbons With CO_2 Ambient

The new EFG ribbons were grown with CO_2 mixed with argon in the ambient as opposed to pure argon for the earlier EFG ribbons. The resistivity was slightly lower, i.e., 0.8 ohm-cm as opposed to 1-2ohm-cm (estimated by zero bias capacitance measurement) of the previous ribbons. The new material was covered by a thin layer of oxidized carbon compound which made an extra surface etching step necessary. Otherwise, the processes used were the same. Baseline cells were fabricated along with earlier EFG material and CZ control silicon for comparison. In addition, some high efficiency cells were fabricated by applying shallow junction diffusion technique, incorporating back surface reflector (BSR) or back surface field (BSF), narrow grid lines, and multi-layer antireflection coating. Appendices in References (1) and (2) provide details of the processes used and reference (3) gives technical details of the EFG process.

EFG Ribbons With CO Ambient

ribbons evaluated had been grown in a furnace with CO-off (Run #18-191-0) and CO-on (Run #18-196-1) atmosphere. The ribbons were sliced into 2x2cm blanks using a dicing saw, and baseline solar cells were fabricated along with CZ silicon (control cell) for comparison.

Other Processes Used

Since significant improvement in solar cell performance, especially short

*Pertinent figures and tables for each section (A,B, etc.) are placed at the end of these sections.and reproduce the tests. circuit current, was reported (4) at

the 1980 European Photovoltaic Solar Energy Conference by utilizing two step diffusion, an experiment was carried out to try and reproduce the tests. Silicon sheets under test were SILSO (Wacker), EFG, and poly silicon from CZ growth. The first step diffusion included 9 hours of $POCl_3$ diffusion at 750°C; it was hoped that preferential diffusion at grain boundaries would occur at this stage. Normal diffusion at 875°C diffusion followed thereafter and baseline solar cells were fabricated. Half of the samples were inserted during the second diffusion (normal 875°C diffusion), serving as control cells, to compare the results of the cells with two step diffusion. No AR coating was applied to these cells.

In an effort to reduce potential residual thermal stress before the cell processing, low temperature annealing was tried on earlier EFG ribbons (Mobil-Tyco Run #187-3C series). The EFG blanks were thoroughly cleaned and annealed at 600°C for 48 hours in nitrogen atmosphere. Baseline solar cells were made from both annealed and un-annealed EFG ribbons and the cell performance was compared to see the effect of the annealing.

2.0 Solar Cell Performance and Characterization

Characteristics Under Illumination

All solar cells were of 2cm x 2cm size. The products from the baseline process had SiO AR coatings and 90% active area with Ti-Pd-Ag metallization. Solar cell parameters such as Isc, Voc, CFF, and n were measured under AM1 conditions at 28°C. Descriptions of the simulator and measurement are given in References (1) and (2).

Parameters of the baseline solar cells from EFG ribbons grown in CO_2 ambient are shown in Table 1, where results of the cells from the earlier EFG

ribbons grown without carbon containing gas atmosphere are also shown for comparison. Note; the two types of the ribbons were processed together.

The new EFG with CO_2 ambient was found to be superior in all parameters, with an average n of 10.3% AM1 as opposed to 8.0% AM1 for the earlier EFG. The slightly lower resistivity of the new EFG would account only partly for the higher Voc values. Other factors such as increased minority carrier diffusion length are needed to account for the rest of the performance difference; this will be discussed later. The results of the high efficiency processes are summarized in Table 2. The best efficiency achieved from the ribbons was 13.8% under AM1 conditions.

The baseline EFG grown in CO ambient showed improvement in all cell parameters, resulting in an average efficiency of 10.7% AM1 compared with 8.6% of the EFG cells without CO in ambient. Table 3 summarizes the results.

Table 4 indicates results of an effort to passivate grain boundaries by two step diffusion (refer to section 1.0 for the details), showing a comparison of short circuit current density Jsc of the solar cells with and without the two step diffusion. Note; Poly CZ and SILSO wafers were processed with EFG. Jsc of poly CZ and SILSO cells stayed about the same, while EFG cells showed reduction in Jsc by the process.

Summary of performance of EFG cells with low temperature annealing are given in Table 5, suggesting the annealing step did not result in improvement of the sheet quality.

Dark Current Characteristics

Dark forward currents were measured. The "A" factor, which is defined by $I_{sc} = I_o (\exp (\frac{qv}{AKT})-1)$, of the baseline samples are listed in Table 6 with their CFF values. The table indicates "A" values equal or more than 2 showing problems of shunting and leading to lower CFF's. All these samples were edge-trimmed so that these values represent leakage in the junction rather than the edge. From the limited number of samples here, it seems that the earlier EFG material is more likely to form leaky junctions. If the high "A" values (>2) are not counted, the rest of the "A" factors with one exception, are within the 1.6-1.8 range both for the new and earlier EFG.

Spectral Response

Spectral response was measured by a filter wheel method (see Reference 1 for the details). Results for selected baseline and high efficiency cells are presented in Figures 1 to 3. It is clear that the new material grown in carbon containing gas atmosphere is superior. Also, a significant enhancement of long wavelength response was noticed in the high efficiency cells. This indicates that the new EFG material responds more positively to BSF or BSR treatments than the earlier EFG. This can be due to longer diffusion lengths (2) as will be seen in the following section.

Minority Carrier Diffusion Length

Effective minority carrier diffusion length (L_D) was measured by the filter wheel method using the short circuit current method (see Reference 1 for the details). Selected samples were measured both in the form of whole samples and at selected areas as shown in the figure attached to Table 7 which gives the results of EFG with CO_2. L_D values of the new EFG range from 30 to 40um

while the earlier EFG ranged from 20 to 30um. This significant increase in L_D is the most decisive factor that accounts for better Isc, because of better carrier collection. Also, the saturation current (I_o) decreases with longer L_D and since $Voc = \frac{AKT}{q} \ln \frac{Isc}{I_o}$; the increase of L_D also accounts for part of the increase of Voc. The light bias effect on L_D for the new EFG has not been studied in this report period. Work in this area will be useful to evaluate the true significance of L_D under one sun illumination.

Table 8 shows results of EFG ribbons with CO ambient, indicating a range of the diffusion length between 35 and 50um for the EFG with CO-on, and 25 and 35um for the EFG with CO-off. L_D of the CZ control cell was about 140um.

Photoresponse by Small Light Spot Scanning

Localized photoresponse of selected solar cells was made using a small light spot scanning technique (see Reference 1 for the detailed description and procedures of the measurement). Figure 4 and Figure 5 show the relative responses of the typical earlier and new EFG, respectively, and also CZ control cells. It is obvious from the presented data that the earlier EFG material has more dips in the response and also has some areas of low response. Chemical etching study in the following section indicates that structural defects are partly responsible for the low response.

Structural Defects

Efforts were made to show structural defects by chemical etching techniques. The etching solution used was diluted Sirtl etch (10 grams of C_2O_3 in 60 ml of deionized distilled water, and an equal volume of concentrated HF). Materials Research Inc. in Utah, reported that 50 seconds in this etching

solution distinctly revealed grain boundaries, twin boundaries, and dislocations for EFG (5). Figure 6 and Figure 7 show microscopic pictures of the etched surface of the earlier and new EFG, respectively; (a) for a typical region and (b) for a area of high dislocation. Dislocation density of the earlier EFG is considerably higher than the new EFG grown in carbon containing gas atmosphere. The earlier EFG also showed areas of dislocation clusters, (b) in Figure 6, which is expected to reduce photoresponse significantly. The low localized response in Figure 4 could possibly be due to this dislocation clusters.

FIGURE 1. SPECTRAL RESPONSE OF BASELINE SOLAR CELLS FROM EFG MATERIAL

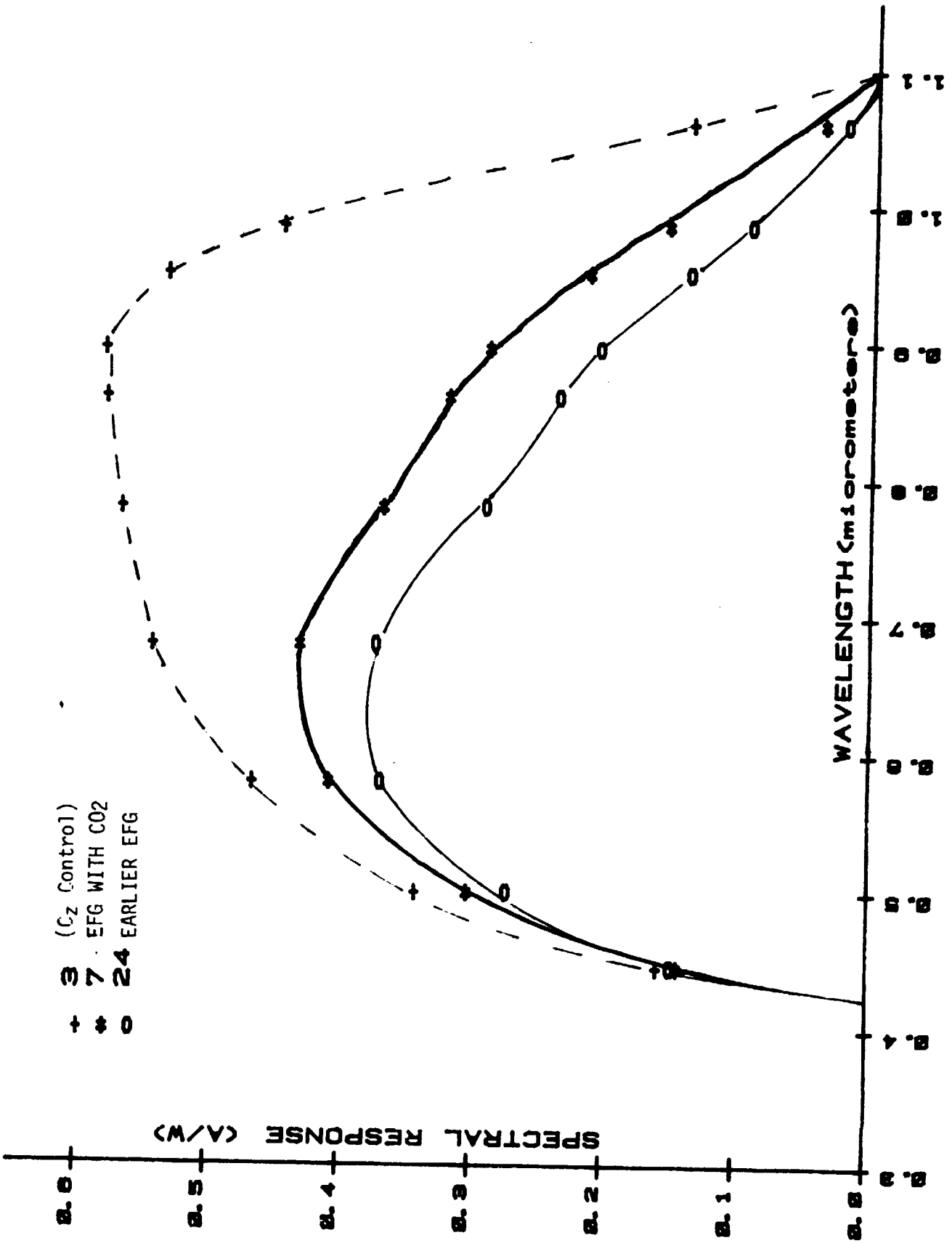

FIGURE 2

SPECTRAL RESPONSE OF THE BASELINE SOLAR CELLS

FROM EFG WITH CO-ON

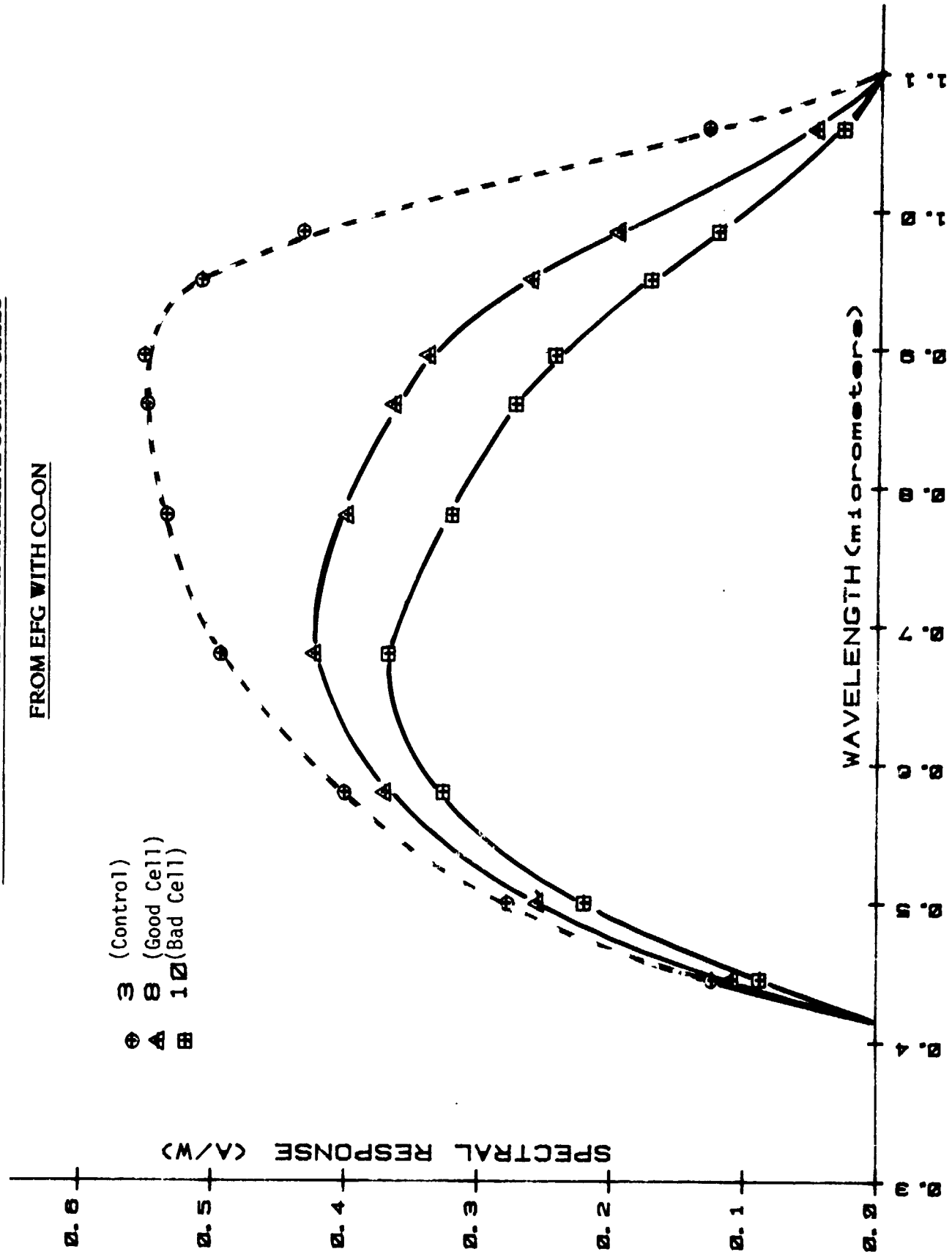

FIGURE 2 (Continued)

SPECTRAL RESPONSE OF THE BASELINE SOLAR CELLS

FROM EFG WITH CO-OFF

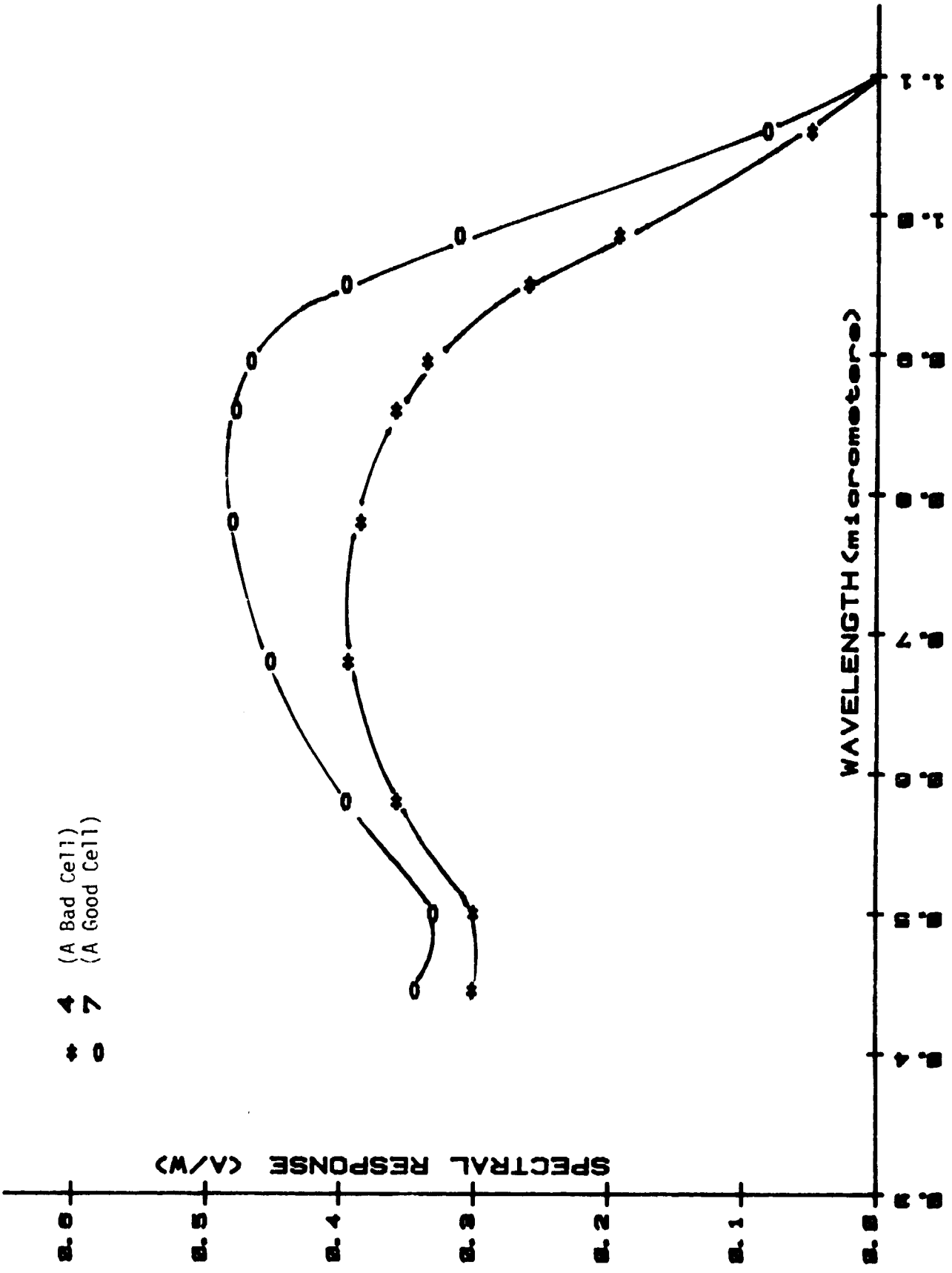

FIGURE 3. SPECTRAL RESPONSE OF HIGH EFFICIENCY SOLAR CELLS FROM EFG RIBBONS (CO_2 AMBIENT)

FIGURE 4. SMALL LIGHT SPOT SCANNING OF TYPICAL EARLIER EFG MATERIAL

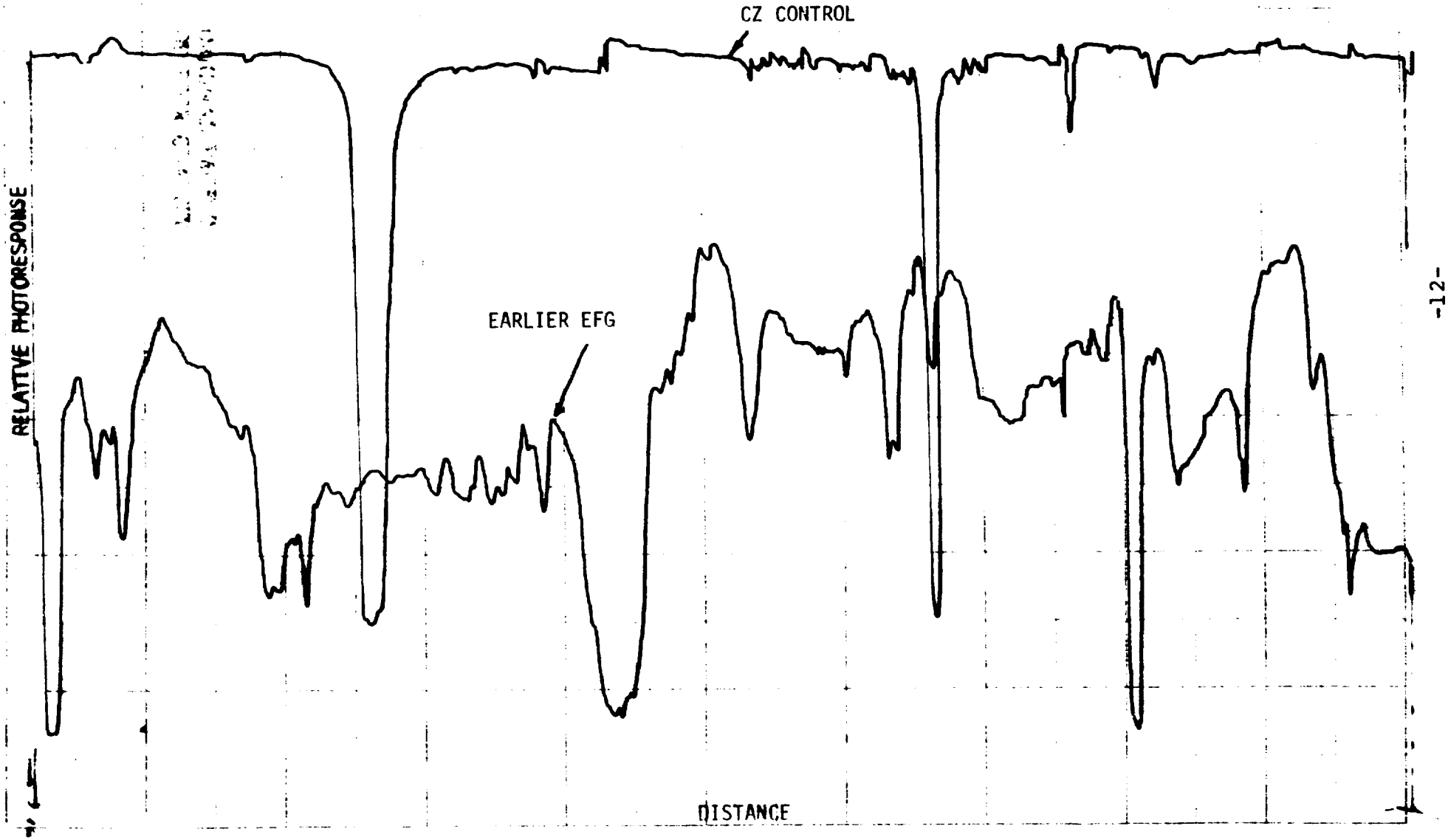

FIGURE 5. SMALL LIGHT SPOT SCANNING OF TYPICAL NEW EFG RIBBONS WITH CO_2

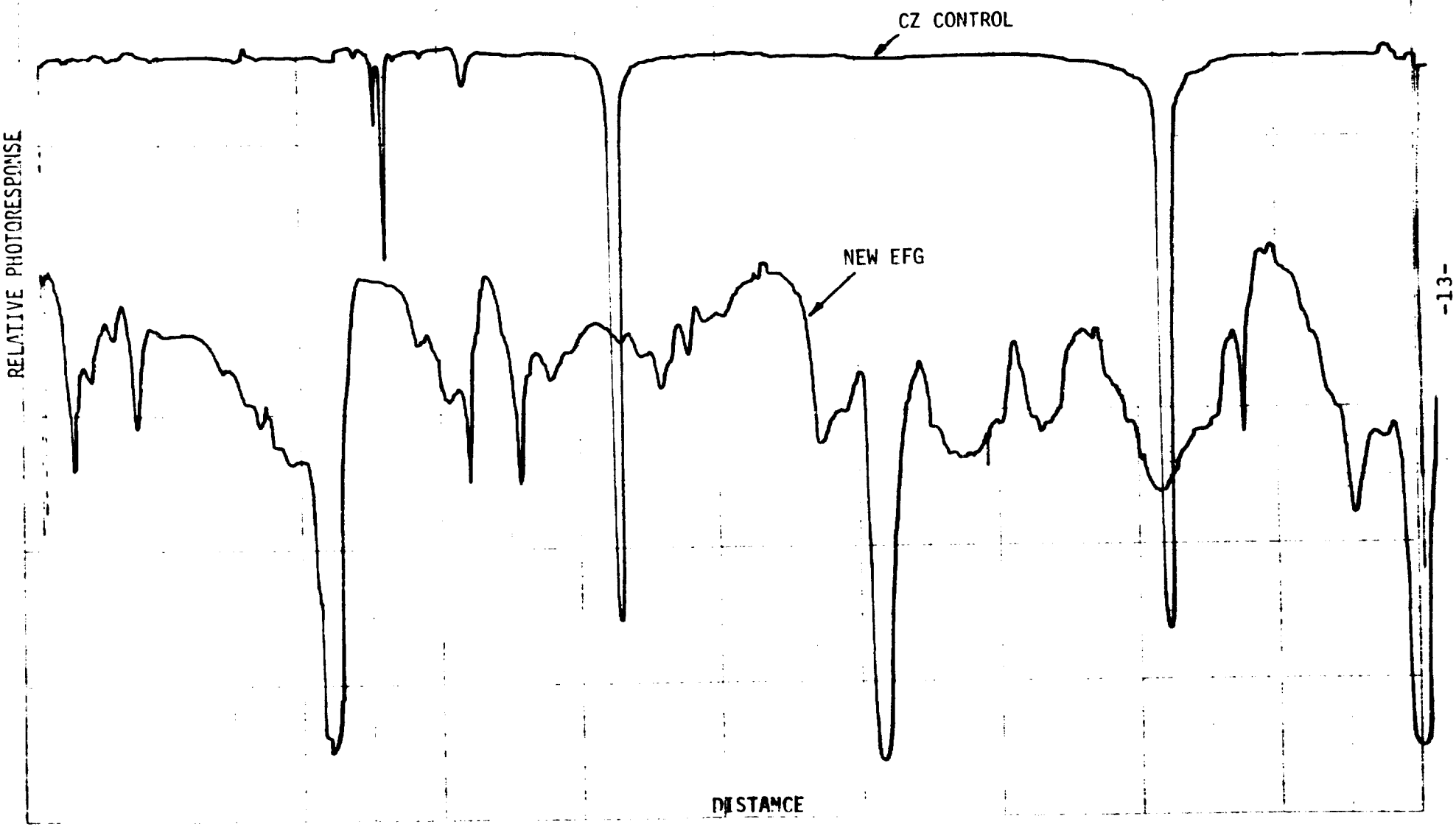

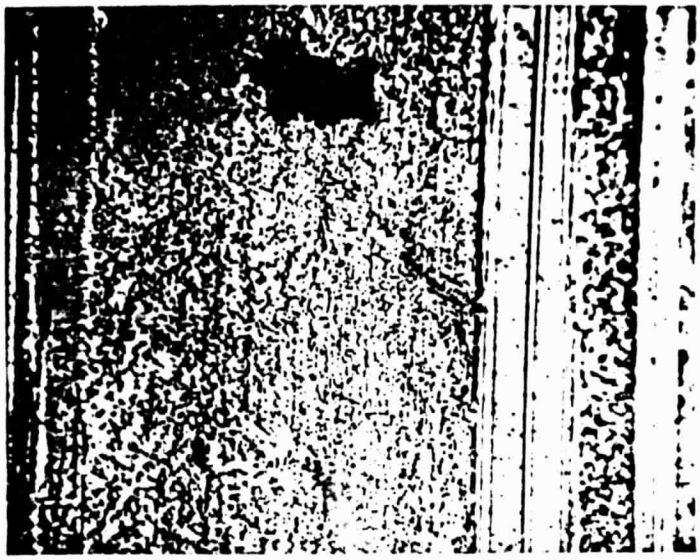

(a) A Typical Area

(b) An Area of High Dislocation Density

FIGURE 6. Microscopic Pictures of the Surface of Earlier EFG After Chemical Etching. (200X Magnification)

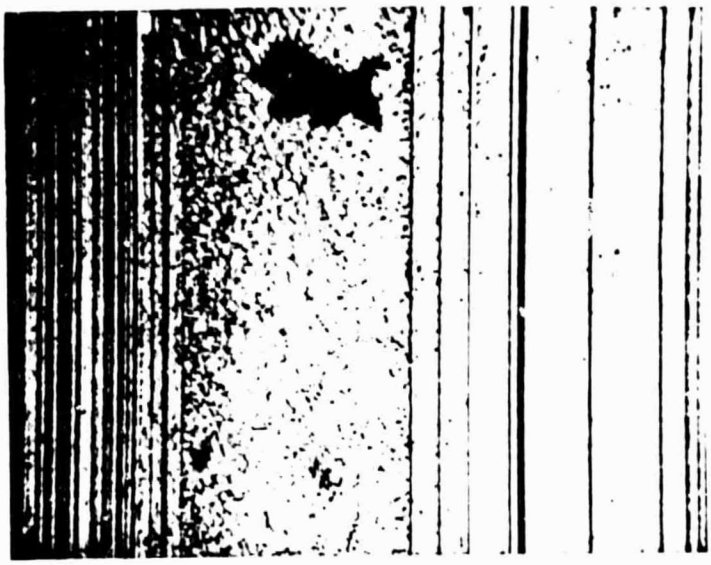

(a) A Typical Area

(b) An Area of High Dislocation Density

FIGURE 7. Microscopic Pictures of the Surface of New EFG With CO_2 Ambient After Chemical Etching (200X Magnification)

TABLE 1

SUMMARY OF BASELINE CELLS FROM EFG RIBBONS WITH CO_2 AMBIENT

		NEW EFG	EARLIER EFG	CZ CONTROL
Voc (mV)	AV.	568	524	588
	S.D.	7	5	-
	R	560~580	516~534	588
Jsc (mA/cm^2)	AV.	24.3	21.4	28.0
	S.D.	.7	.8	-
	R	23.0~25.0	20.5~23.0	27.8~28.3
CFF (%)	AV.	75	71	76
	S.D.	3	3	-
	R	69~77	65~75	75~77
η (%)	AV.	10.3	8.0	12.6
	S.D.	0.6	0.4	-
	R	9.6 ~ 11.1	7.4 ~ 8.7	12.3 ~12.8

NOTE: 1) 2x2 cm Cells with SiO AR coating measured under AM1 at 28°C test block temperature.

2) New EFG: Improved grains, grown in CO_2 gas atmosphere.

TABLE 2

SUMMARY OF HIGH EFFICIENCY CELLS FROM NEW EFG RIBBONS WITH CO_2 AMBIENT

	Voc (mV)	Jsc (mA/cm^2)	CFF (%)	(%)
AV.	565	28.4	76	12.1
S.D.	9	1.1	2	.7
R	550-574	27.0-30.3	72-78	11.5-13.6

(a)

Voc (mV)	Jsc (mA/cm^2)	CFF (%)	η (%)
578	30.3	79	13.8

(b)

NOTE: 1) 2x2 cm cells with AR coating at 28°C test block temperature under AM1 conditions.

2) Process Used:
   (a) SJ,BSR, and MLAR.
   (b) SJ, BSF, and MLAR.

TABLE 3

AVERAGE CELL PARAMETERS OF EFG RIBBONS WITH AND WITHOUT CO IN AMBIENT

	Voc, mV	Jsc mA/cm^2	CFF, %	η, %
WITHOUT CO	540	22.9	70	8.6
WITH CO	567	25.1	76	10.7
CZ CONTROL	582	28.2	78	12.7

NOTE: Baseline Solar Cells (2x2cm) With SiO AR Measured at $28^{\circ}C$ Under AM1.

TABLE 4

AVERAGE SHORT CIRCUIT CURRENT DENSITY (Jsc, mA/cm^2)
FOR TWO STEP DIFFUSION PROCESS (750^oC, 9Hr. in $POCl_3$)

	EFG	POLY HAMCO	SILSO
No 2 Step Diffusion	17.9	22.1	22.4
2 Step DIFFUSION	15.3	22.1	22.3

Jsc of Control: 23.4

Baseline process on 2x2 cells without AR, measured at AM1, 28^oC. (EFG material without CO in growth)

TABLE 5

EFG MATERIAL WITH LOW TEMPERATURE ANNEALING (600°C,30 Hr)

	Voc,mV	Jsc_2 mA/cm	CFF %	η %
NOT ANNEALED	493	13.2	74	4.8
ANNEALED	493	13.3	73	4.7
CZ CONTROL	568	20.1	74	8.5

BASELINE PROCESS ON 2x2 CELLS WITHOUT AR MEASURED AT AM1 AT 28°C. (EFG MATERIALS GROWN WITHOUT CARBON CONTAINING GAS ATMOSPHERE)

TABLE 6

"A" FACTORS FROM DARK I-V MEASUREMENTS

	CELL NOS.	A	CFF
NEW EFG WITH CO_2 AMBIENT	1	1.71	.77
	2	1.69	.75
	7	1.69	.76
	9	1.62	.75
	11	2.05	.70
	12	1.75	.74
EARLIER EFG	14	1.79	.73
	16	2.14	.69
	17	1.63	.72
	19	2.0	.70
	21	1.7	.75
	22	1.45	.74
	23	1.73	.74
CZ CONTROL	C-3	1.83	.75
	C-4	1.27	.78

TABLE 7

EFFECTIVE MINORITY CARRIER DIFFUSION LENGTHS OF EFG RIBBONS WITH CO_2

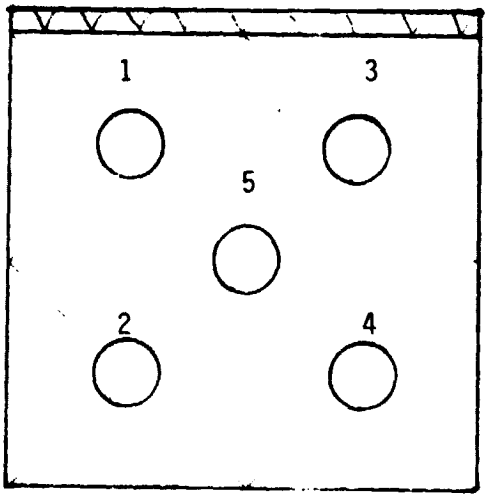

Diameter of the Circle = 3mm

	DIFFUSION LENGTH (μm)					
	WHOLE	1	2	3	4	5
Cz Control C-3	119	119	120	126	126	120
New EFG (CO_2) #7	40	50	48	40	40	34
New EFG (CO_2) #13	28	26	25	18	23	34
EARLIER EFG #16	18	14	24	18	20	17
EARLIER EFG #24	28	34	30	32	34	19

TABLE 8

EFFECTIVE MINORITY CARRIER DIFFUSION LENGTH OF SELECTED SOLAR CELLS FROM EFG RIBBONS WITH AND WITHOUT CO IN AMBIENT

	EFG WITH CO		EFG WITHOUT CO		CZ CONTROL
CELL I.D.	#8	#10	#7	#3	
DIFFUSION LENGTH (um)	50	35	35	25	140

NOTE: Diffusion Length (effective) Measured on Whole Area (2x2cm) Using Short Circuit Current Method.

B. Dendritic Web Solar Cells

1.0 Solar Cell Fabrication

Blank shaping (2x2cm) and removal of the surface deposit (SiO) were carried out using the same method described in Section E of Reference (1). Baseline solar cells were fabricated from dendritic webs for various runs; Run 17-1373 (J176-213, 8.5 ohm-cm), 17-1377 (J220-2.6, 3.4 ohm-cm), and 17-1390 (J183-1.5, 9.4 ohm-cm). Efforts were made to improve the performance by forming a shallow junction, using fine grid lines, BSF and MLAR coating. Baseline solar cells were also fabricated from the same webs and the results were compared. Dendritic webs tested were #17-1387 (J180-2.7, 8 ohm-cm), 17-1388 (J181-3.7, 11 ohm-cm), 17-1389 (J181-3.8, 11ohm-cm), 17-1402 (AA009-4.4, 3 ohm-cm).

Baseline solar cells were also fabricated on 2x2 wafers pre-characterized in terms of dislocation density by MRI (Utah), in an effort to correlate solar cell parameters with defects. Table 9 shows dislocation densities provided by MRI. The table indicates there is no significant difference in dislocation count between the samples. See Reference (6) for the details of the Web process.

2.0 Solar Cell Performance and Characterization

Characteristics Under Illumination

Finished solar cells were tested under AM1 condition at 28°C test block temperature. Table 10 summarizes cell parameters of the baseline process, indicating an average efficiency slightly higher than 11% for dendritic web cells. NOTE: The average efficiency of the CZ control cells (starting substrate resistivity of 1-3 ohm-cm) was about 13%. Lower efficiency of the web cells was mainly due to lower open circuit voltage, caused by the higher starting

substrate resistivity of the webs. Short circuit current density of the web cell was lower than the control cells, (by about $1mA/cm^2$) suggesting that the quality of the webs under investigation is not quite so good as that of conventional CZ silicon. Cell parameters from the advanced process are summarized in Table 11, showing an average efficiency of 12.5% which is an efficiency improvement of about 1% over the baseline solar cells. Open circuit voltage enhancemnent by the BSF process does not seem to be as effective as in earlier tests. The reason for the small improvement in Voc is not known at present.

For the pre-characterized cells, list in Table 9, baseline solar cell parameters are summarized in Table 12. As expected, no significant difference in various parameters is indicated. The average efficiency was about 10.8% AM1 which is a slightly lower value than that of the CZ control cells of similar substrate resistivity, mainly due to lower Jsc.

Spectral Response

Absolute spectral response (A/W) was obtained using a filter wheel set-up. The results are plotted in Figure 8 for the baseline solar cells. The web cells show response close to those of the CZ control cells, yet showing slightly lower response in the long wavelength region.

Minority Carrier Diffusion Length

Minority carrier diffusion length (L_D) was measured by the filter wheel method using the short circuit current method. Selected samples were measured by illuminating the whole area. The results showed values of about 130um for #6 cell (from web I.D.#17-1373), and 110um for #14 cell (from web I.D. #17-1377), while L_D of the CZ control cell indicated about 150um.

The results of the samples from the pre-characterized webs are listed in Table 13 and they are quite uniform. The whole range of variation was between 58 and 68um which agrees well with the MRI data in terms of defect counts.

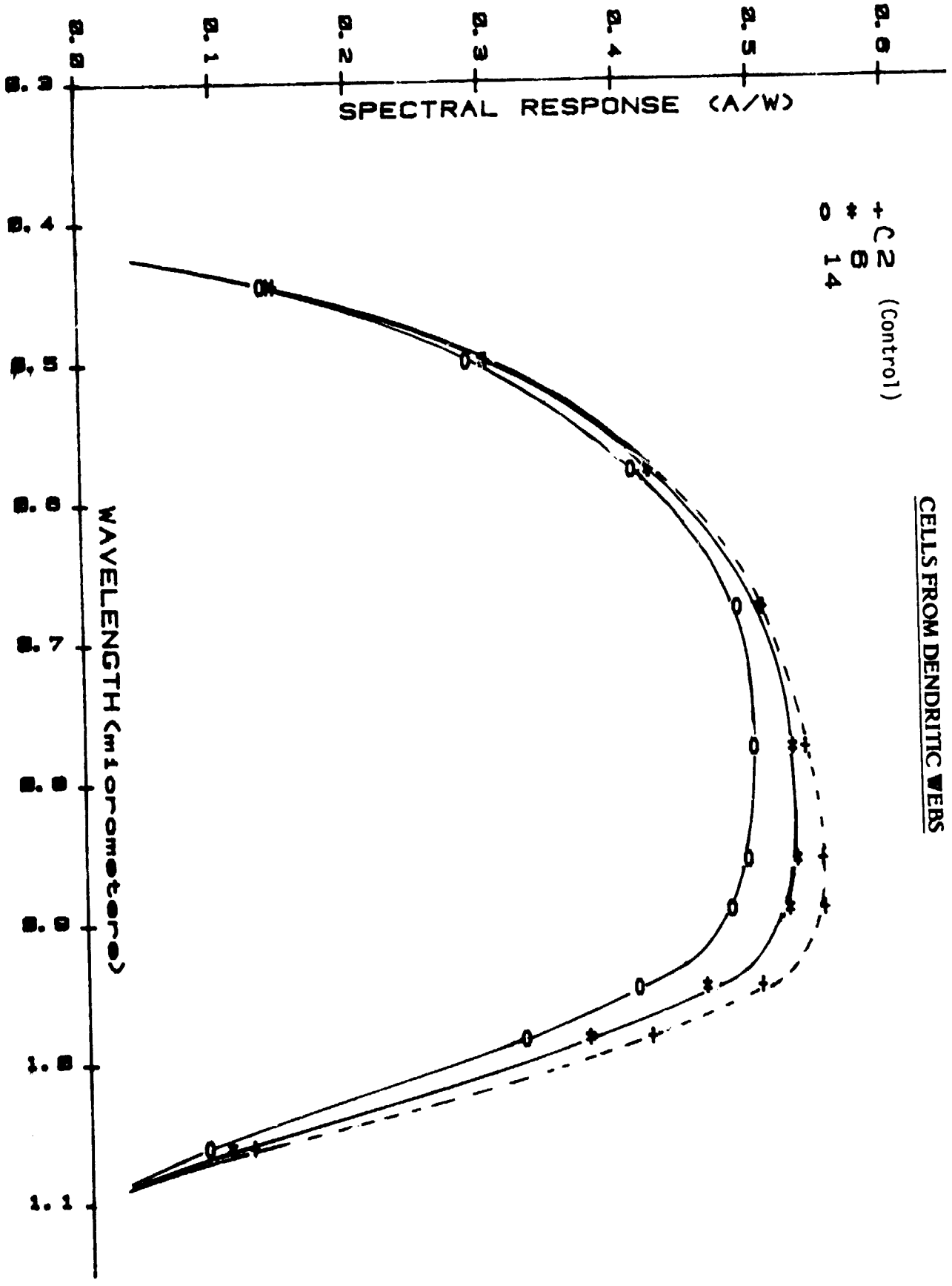

FIGURE 8

SPECTRAL RESPONSE OF THE BASELINE SOLAR CELLS FROM DENDRITIC WEBS

TABLE 9

ANALYSIS OF DENDRITIC WEB SAMPLES

JPL SAMPLE #	NO. OF DISLOCATIONS PITS/FIELD	NO. OF DISLOCATIONS PITS/um^2
J250-4.7-A	17.808	2.737×10^{-4}
J250-4.7-B	14.946	2.298×10^{-4}
J250-4.7-C	12.146	1.867×10^{-4}
J250-4.7-D	16.614	2.554×10^{-4}
J250-4.7-E	15.526	2.387×10^{-4}
J250-4.7-F	15.800	2.429×10^{-4}
J250-4.7-K_1	15.828	2.433×10^{-4}
J250-4.7-K_2	16.615	2.554×10^{-4}
J250-4.7-L_1	37.424	5.753×10^{-4}
J250-4.7-L_2	27.082	3.702×10^{-4}

TABLE 10

DENDRITIC WEB SOLAR CELL FROM BASELINE PROCESS

		WEB I.D. NO.			CZ CONTROL
		17-1373 ρ=8.5 Ω-cm	17-1377 ρ=3.4Ω-cm	17-1390 ρ=9.4Ω-cm	
Voc (mV)	AV.	532	534	515	588
	S.D.	530~534	532~536	512~518	584~590
	R	2	2	3	3
Jsc (mA/cm^2)	AV.	28.8	28.1	28.6	29.8
	S.D.	0.5	0.3	0.5	0.5
	R	28.3~29.4	27.8~28.4	27.4~29.0	29.3~30.0
CFF (%)	AV.	76	76	75	74
	S.D.	1	1	1	3
	R	75~76	75~76	74~77	70~76
η (%)	AV.	11.6	11.4	11.0	13.0
	S.D.	0.1	0.1	0.2	0.6
	R	11.4~11.7	11.3~11.5	10.6~11.3	12.2~13.5

NOTE: 1) 2x2 cm cells under AM1 measured at 28°C test block temperature.

2) CZ Control Cells: 1-3 ohm-cm

TABLE 11

DENDRITIC WEB SOLAR CELLS FROM ADVANCED PROCESS

			CONTROL CELLS (NO BSF)	
		WEB	WEB	CZ
Voc (mV)	AV.	545	531	581
	S.D.	14	11	-
	R	582-558	514-546	578-582
Jsc (mA/cm^2)	AV.	29.2	28.1	29.9
	S.D.	0.6	0.5	-
	R	28.5-29.8	27.4-28.8	29.3 - 30.4
CFF (%)	AV.	79	78	78
	S.D.	1	1	1
	R	78-80	75-79	77-79
η (%)	AV.	12.5	11.7	13.5
	S.D.	0.6	0.5	-
	R	11.8-13.0	10.9 - 12.2	13.2 - 13.7

NOTE: 1) Measured under AM1 at 28°C test block temperature.

2) Advanced process: SJ+BSF+MLAR

3) CZ Control Cells: 1-3 ohm-cm

TABLE 12

SUMMARY OF THE PRE-CHARACTERIZED WEB WAFERS

	Voc (mV)	Jsc (mA/cm^2)	CFF (%)	η (%)
AVERAGE	534	26.3	77	10.8
STANDARD DEVIATION	1	.1	1	.2
RANGE	532-534	26.2-26.5	76-78	10.6-10.8

TABLE 13

MINORITY DIFFUSION LENGTHS OF THE PRE-CHARACTERIZED WEB CELLS

SAMPLE I.D.	L_D(um)
C	65
T2	62
F	58
K-1	62
K-2	63
L	62
Control #11	121

C. Solar Cells From Cast Silicon Ingots by Heat Exchanger Method (HEM)

Four HEM cast silicon ingots were evaluated during the contract period; a cast cube section (4"x4"x 4", Crystal System ID #41-07), a small cast ingot (~6"x 6"x 4", Crystal System ID #41-24), and two large cast ingots (~12"x 12"x 6", Crystal System ID #'s 41-41C and 41-48).

The crystals used semiconductor grade starting materials, and the purpose of the study was to test material uniformity by measuring solar cell performance as a function of the positio in the crystals. Reference (7) provides technical details of the HEM process.

1.0 Solar Cells From A Cube Section (#41-07)

Solar Cell Fabrication

The cube was cut horizontally with respect to its casting position (refer to Figure 9 for wafer preparation) and wafers were marked relative to the top of the ingot. The ingot was mostly single crystal and measurement of the resistivity indicated about 2 ohm-cm with P-type conductivity. 2x2 blanks were cut from the ingot and they were all marked such that their positions were traceable. Baseline process was applied to fabricate cells and for some of the cells, an extra step of gettering by diffusion glass was applied before the baseline process. Also, an attempt to anneal the wafers was made on some samples before the baseline process. Because this crystal showed a clear correlation between performance and position, high efficiency processing (including gettering, shallow junction with narrow grid lines, BSF, MLAR) was applied to the best portion of the crystal.

*In Section C, figures and tables are placed at the ends of sub-sections 10, 20, etc., since these subsections are fairly long.

Characteristics Under Illumination

Solar cells made by the baseline process had 90% active area and SiO AR coating while high efficiency cells had 94% active area and MLAR coating. Solar cell parameters such as Voc, Isc, CFF, and n were measured at 28°C under AM1 conditions (see Reference 1 for description of simulator). In order to illustrate the relations between solar cell performance and position within the crystals, Figure 9 gives average solar cell efficiency (using the baseline process) as a function of position. It is obvious that a definite pattern can be established; best solar cell performance is found in the upper middle portion of the crystal, the top portion is slightly inferior, and performance deteriorates in the lower half with the worst cells close to the seed. After gettering treatment, most improvement was found in the lower middle portion of the crystal. Annealing at 600°C made no significant improvement in cell performance. For the best portion of the crystal, cell performance, whether baseline process or high efficiency process is comparable to the single crystal CZ controls. The result of high efficiency processing is given in Table 14. Also, no significant deviation was detected between the edge and center portions of any wafer, nor between polycrystalline and single crystalline portions. For this horizontally cut (#41-07) crystal, the only positional variable was the distance from the bottom surface.

Spectral Response

Absolute spectral response (A/W) was obtained using a filter wheel set-up. Figures 10 to 12 show the response of selected samples of baseline, gettered + baseline, and high efficiency processes for samples from the horizontally cut crystal (#41-07).

Light Bias Minority Carrier Diffusion Length Measurement

The varying performance of solar cells from different portions of HEM crystals indicate the possibility of existence of recombination centers in the low performance positions. Light bias minority carrier diffusion length measurements should indicate their existence. Selected samples from both crystals were measured by the SSI 100 diffusion length meter which has a built in light bias source.

The difference between the SSI system and a filter wheel is that the SSI can only measure a relatively small localized area of the solar cell. The bias source was a tungsten-halogen lamp. The bias level varied from approximately 1/3 sun to 6.8 suns. The results are shown in Figure 13. The cells with lower L_D showed higher relative increase in L_D with illumination. Also observed were photondegradation effect in some of the cells as indicated by cell 2-3.

DLTS Measurements

In order to look at the defect structure from a different direction, some preliminary deep level transient spectroscopy (DLTS) measurements for the horizontally cut crystals were made. The DLTS system used (reference #8 for the DLTS system) belongs to JPL. Not enough measurements were made to achieve consistency of the results. However, preliminary indications were that extra distributions of defect levels existed in the lower portion of the crystal (8 and 12 series) while these levels could not be found in the upper portion (5 and 2 series). This is consistent with the light bias results. There is also some indication that a common defect level exists in all cells.

FIGURE 9. AVERAGE EFFICIENCY vs. POSITION OF THE HORIZONTALLY CUT HEM CUBE (BASELINE PROCESS) (HEM CUBE #41-07)

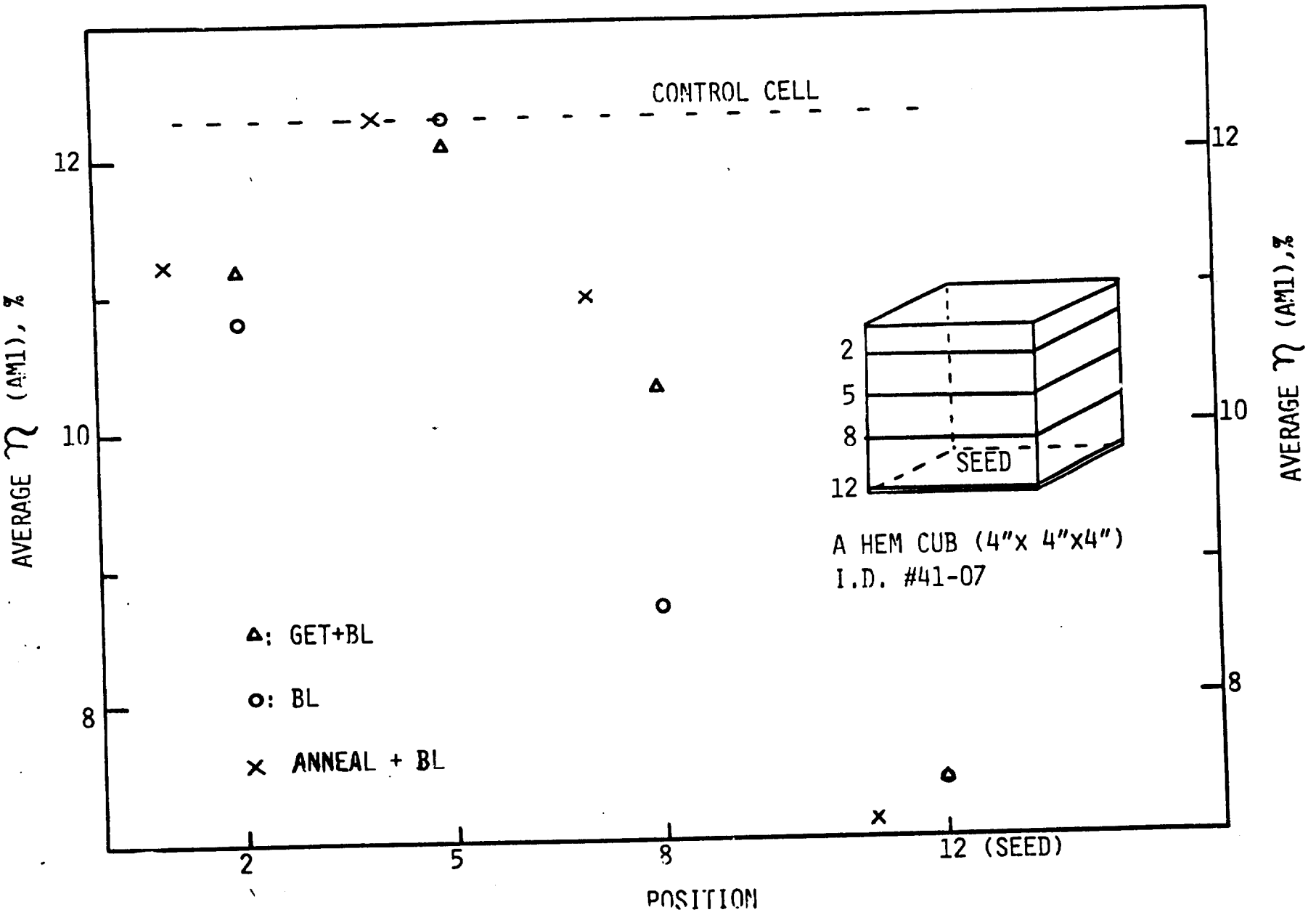

FIGURE 10 (A). SPECTRAL RESPONSE OF SOLAR CELLS FROM A HEM CUBE (#41-07)
BASELINE PROCESS

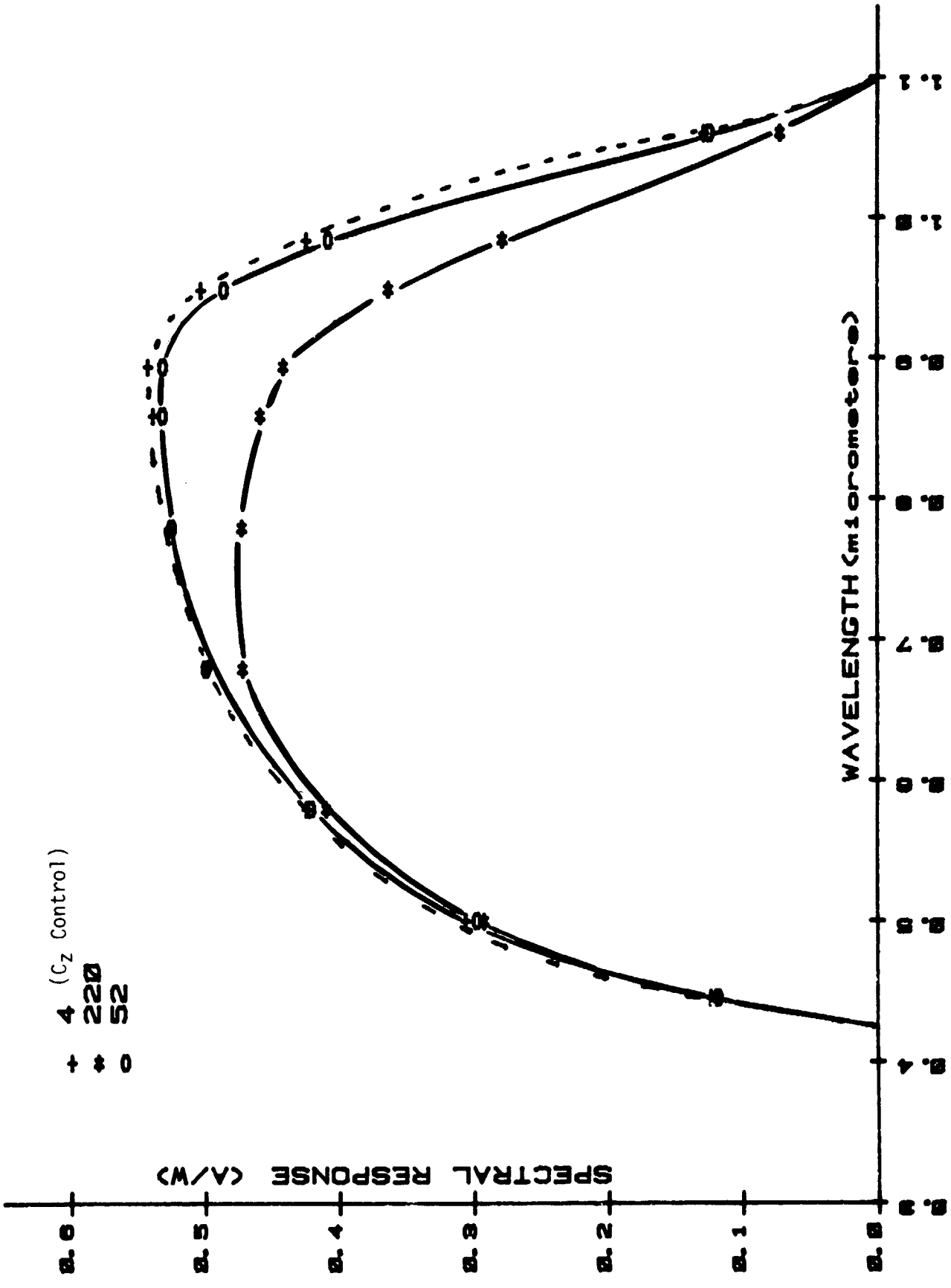

FIGURE 10 (B). SPECTRAL RESPONSE OF SOLAR CELLS FROM HEM CUBE (#41-07)
BASELINE PROCESS (Continue)

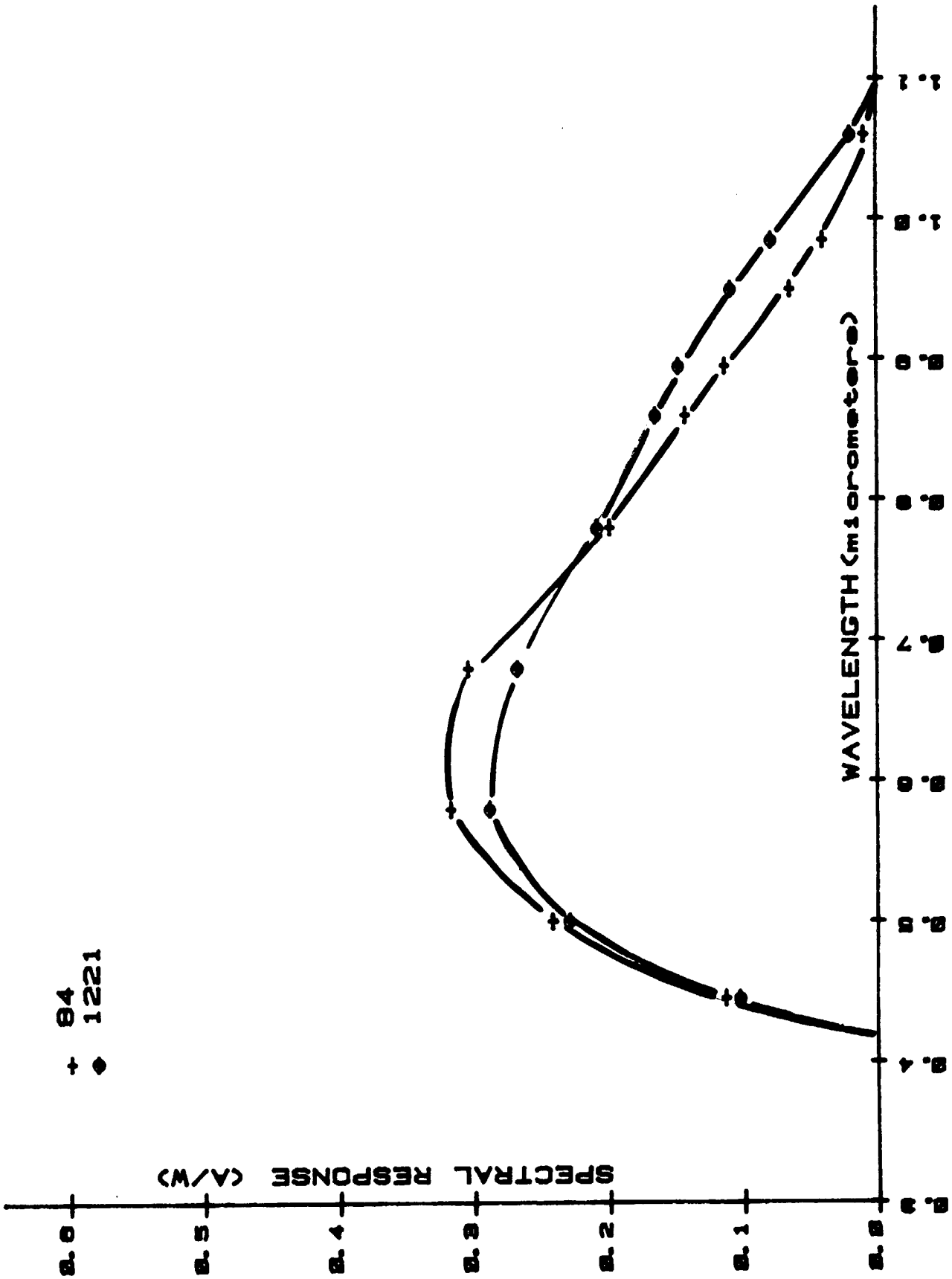

FIGURE 11 (A). SPECTRAL RESPONSE OF SOLAR CELLS FROM A HEM CUBE (#41-07)
GETTERING + BASELINE PROCESS

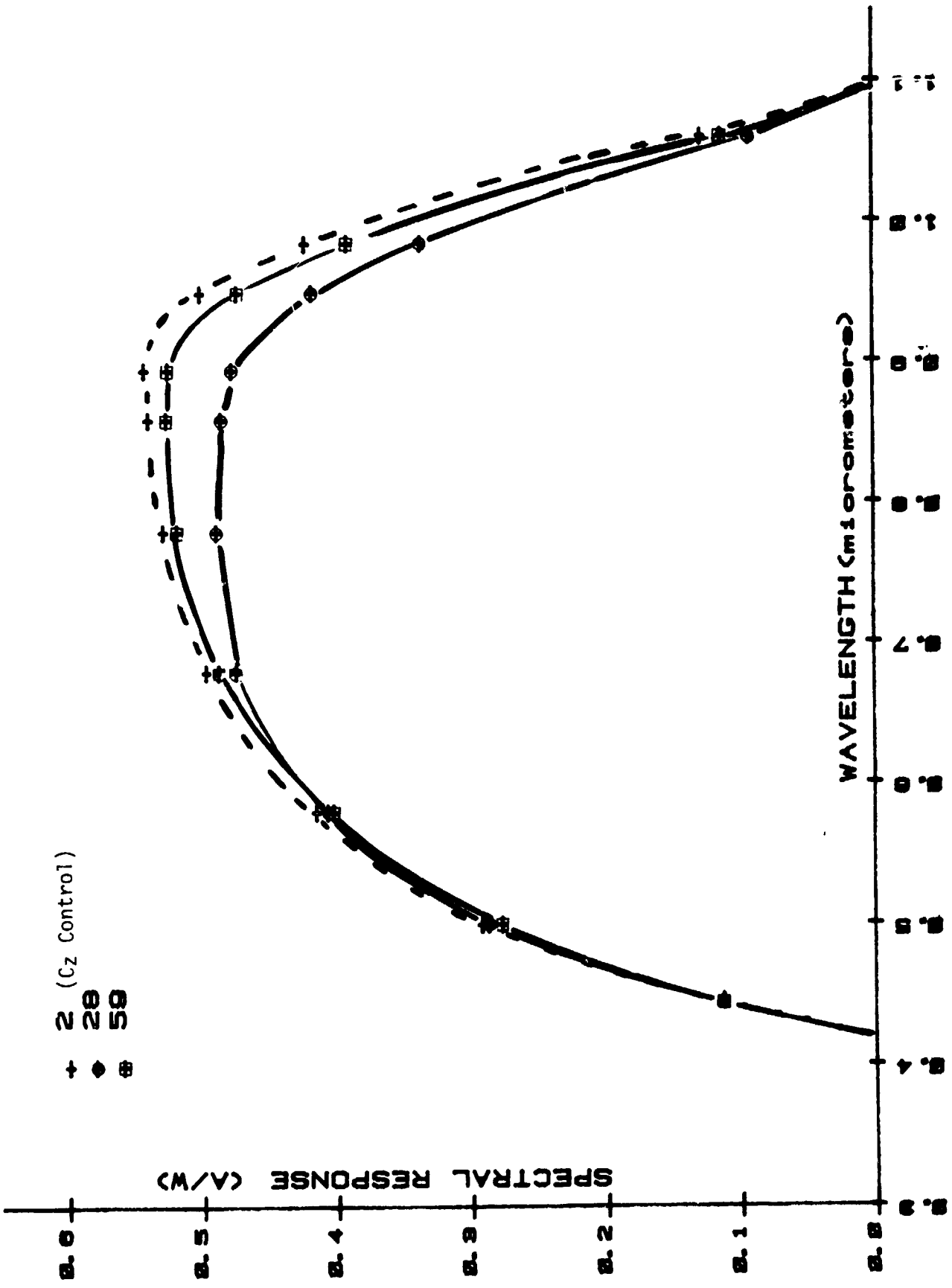

FIGURE 11 (B). SPECTRAL RESPONSE OF SOLAR CELLS FROM A HEM CUBE (#41-07) GETTERING + BASELINE PROCESS (Continue)

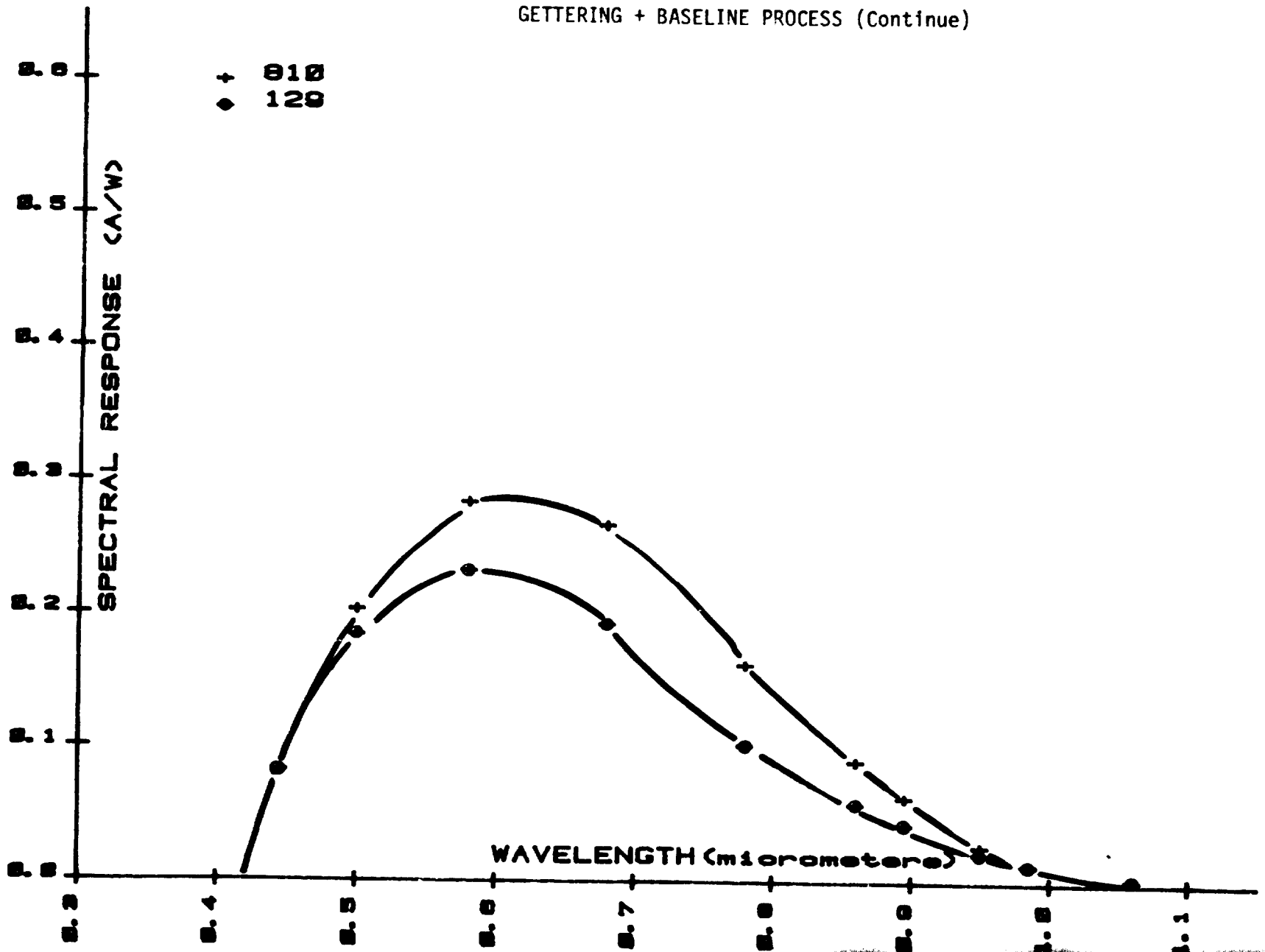

FIGURE 12. SPECTRAL RESPONSE OF SOLAR CELL FROM HEM CUBE (#41-07)
GET, SJ, NARROW GRIDLINES, BSF, MLAR PROCESS

FIGURE 13

L_D's vs. No. of Suns for Horizontally Cut HEM Cube Cells (#41-07)

(Cells No. in Parenthessis)

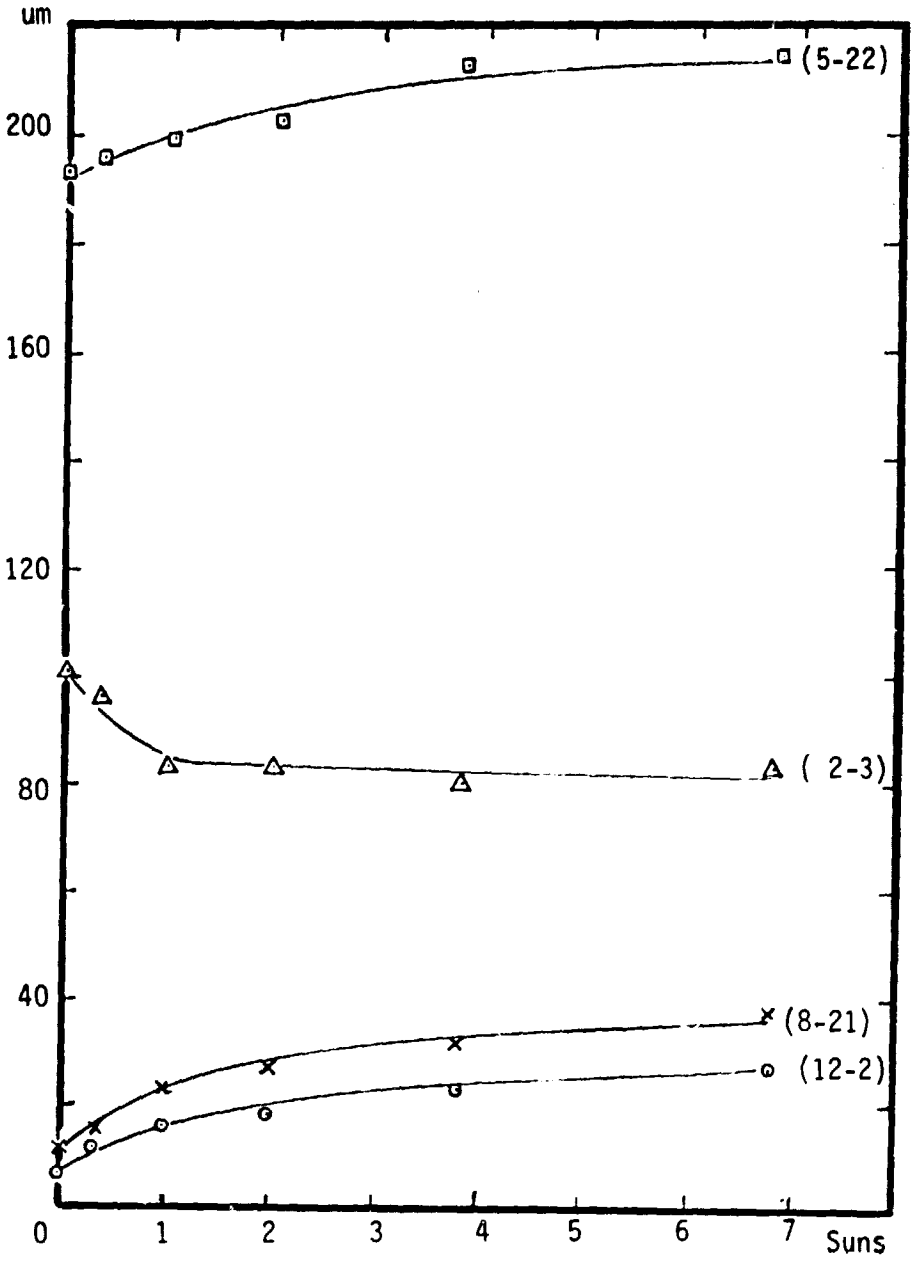

TABLE 14

SUMMARY OF HIGH EFFICIENCY CELLS FROM A SELECTED PORTION OF A HEM INGOT (#41-07)

	Voc (mV)	Jsc (mA/cm^2	CFF (%)	η (%)
AV	597	32.4	78	15.0
S.D.	3	.6	2	.5
R	588-602	30.6-33.3	75-80	13.5-15.7

NOTE:
1) 2x2 cm cells with AR coating measured under AM1 at $28^{o}C$ test block temperature.
2) Solar cells were fabricated from a portion of the ingot (#41-07), where good baseline performance was obtained.
3) Processes used were Gettering, SJ, BSF, and MLAR.

2.0 Solar Cells From A Small Cast Ingot (#41-24)

Solar Cell Fabrication

A whole cast ingot was cut vertically with respect to casting position and only central parts of the crystal were used for evaluation (Figure 14 for the details). 2x2cm silicon blanks were prepared from the wafers and baseline solar cells were fabricated.

Gettering by diffusion glass was also carried out. Two gettering experiments were made; one on the cleaned saw-cut wafers and the other on the chemically polished wafers.

Characteristics Under Illumination

Finished baseline solar cells had no AR coating and about 90% active area with Ti-Pd-Ag metallization. Solar cell parameters, such as Isc, Voc, CFF, and n, were measured under an AM1 conditions at 28^{o}C test block temperature.

Figure 15 to 18 show mappings of the solar cell parameters; a definite pattern cannot easily be established. Judging from Isc (Figure 15) it seems that the edges except on the bottom section are lowest and across the ingot the upper middle portion is the worst section. (Only slight deterioration occured close to the seed in contrast to the horizontally cut crystal.) All the cells were inferior to the CZ control cells.

Normalized efficiencies of the baseline (with respect to the CZ controls) HEM cells with the gettering process are shown in Figure 19. The result suggested; 1) dependence of cell performance on the location is similar with the

baseline process, and 2) no significant improvement in cell performance was noticed after the gettering.

Minority Carrier Diffusion Length

Light bias minority carrier diffusion length was carried out using the same method described in section 1.0. The results of the selected samples are plotted in Figure 20, indicating similar results with the cells fromthe cube (#41-07).

FIGURE 14

CROSS SECTION OF A VERTICALLY CUT HEM INGOT

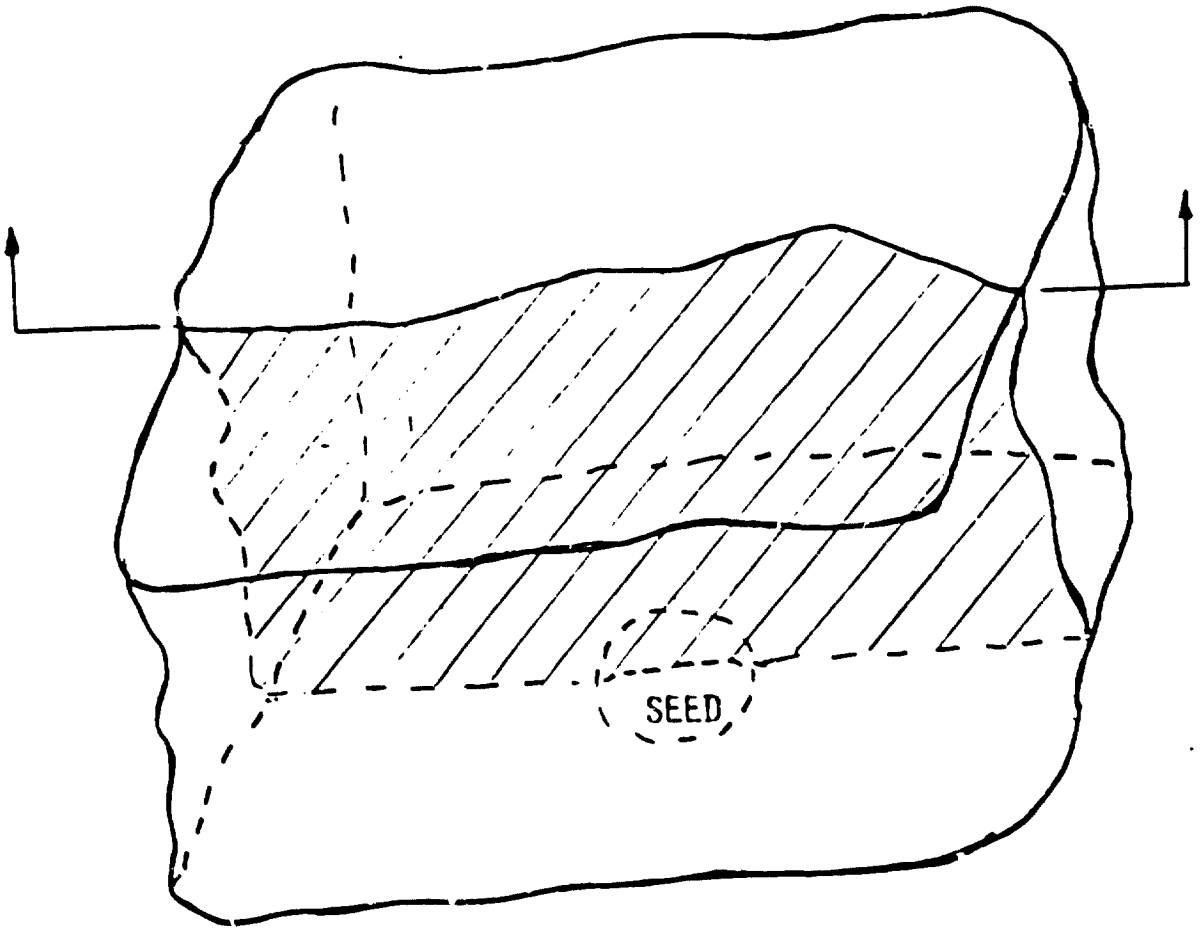

A HEM INGOT (ID #41-24)

FIGURE 15

SHORT CIRCUIT CURRENT DENSITY (AM1, NO AR) MAPPING OF A VERTICALLY CUT HEM WAFER FROM A CAST INGOT (#41-24)

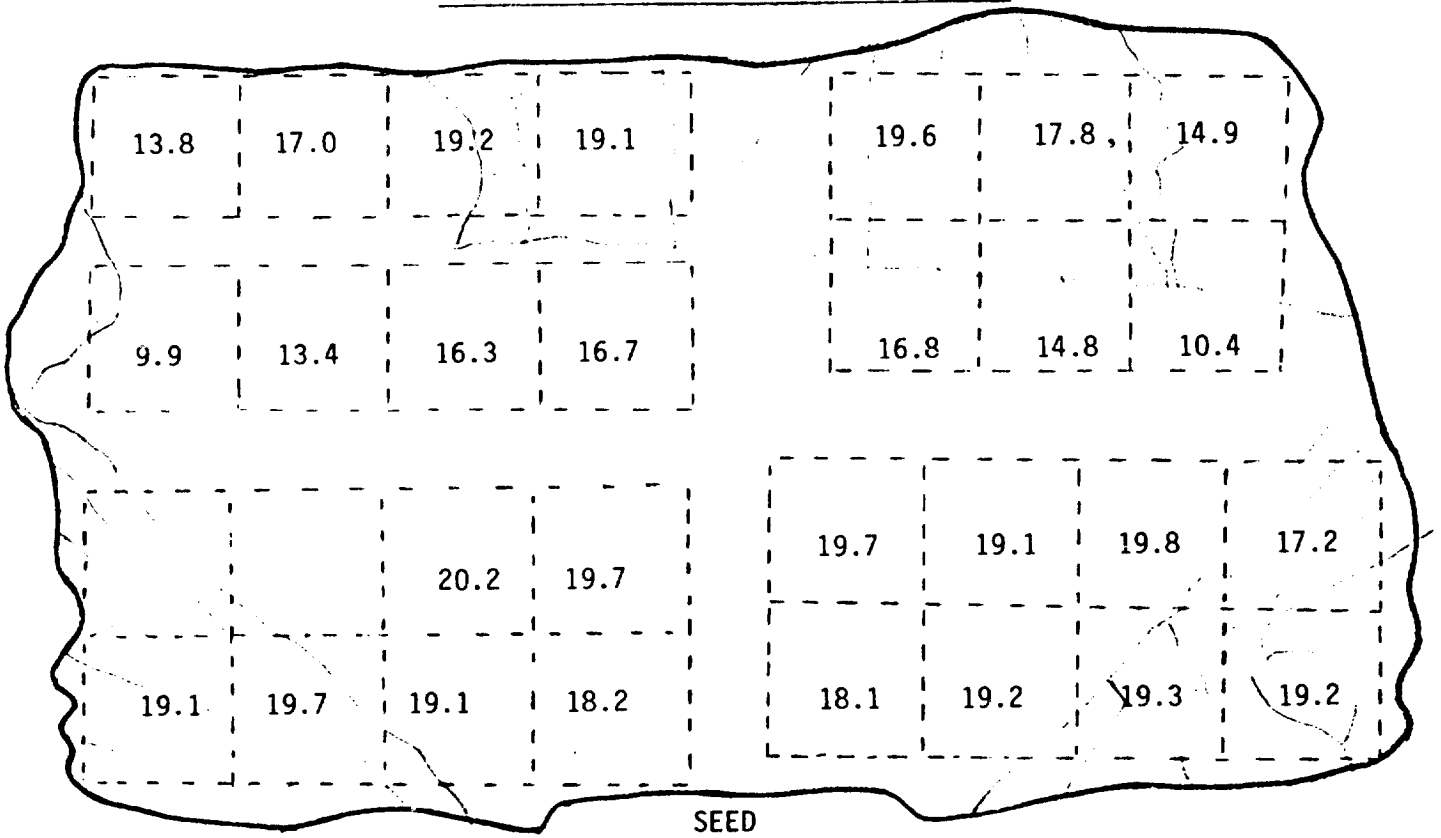

NOTE: UNIT: mA/cm^2

Jsc OF CONTROL CELL = 21.3 mA/cm^2

FIGURE 16

OPEN CIRCUIT VOLTAGE (AM1, NO AR) MAPPING OF A VERTICALLY CUT HEM WAFER FROM A CAST INGOT (#41-24)

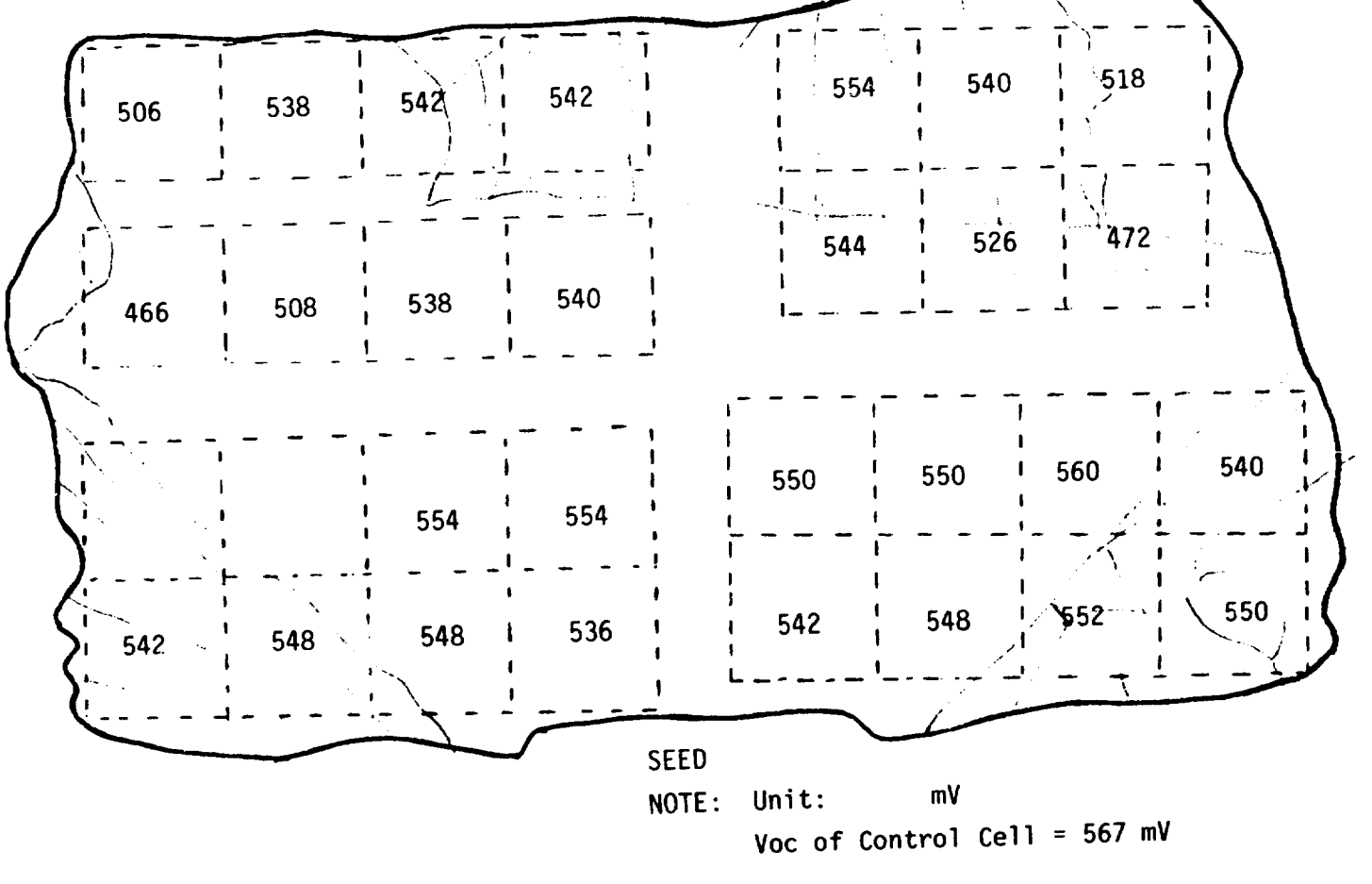

NOTE: Unit: mV

Voc of Control Cell = 567 mV

FIGURE 17

EFFICIENCY (AM1, NO AR) MAPPING OF A VERTICALLY CUT HEM WAFER FROM A CAST INGOT (#41-24)

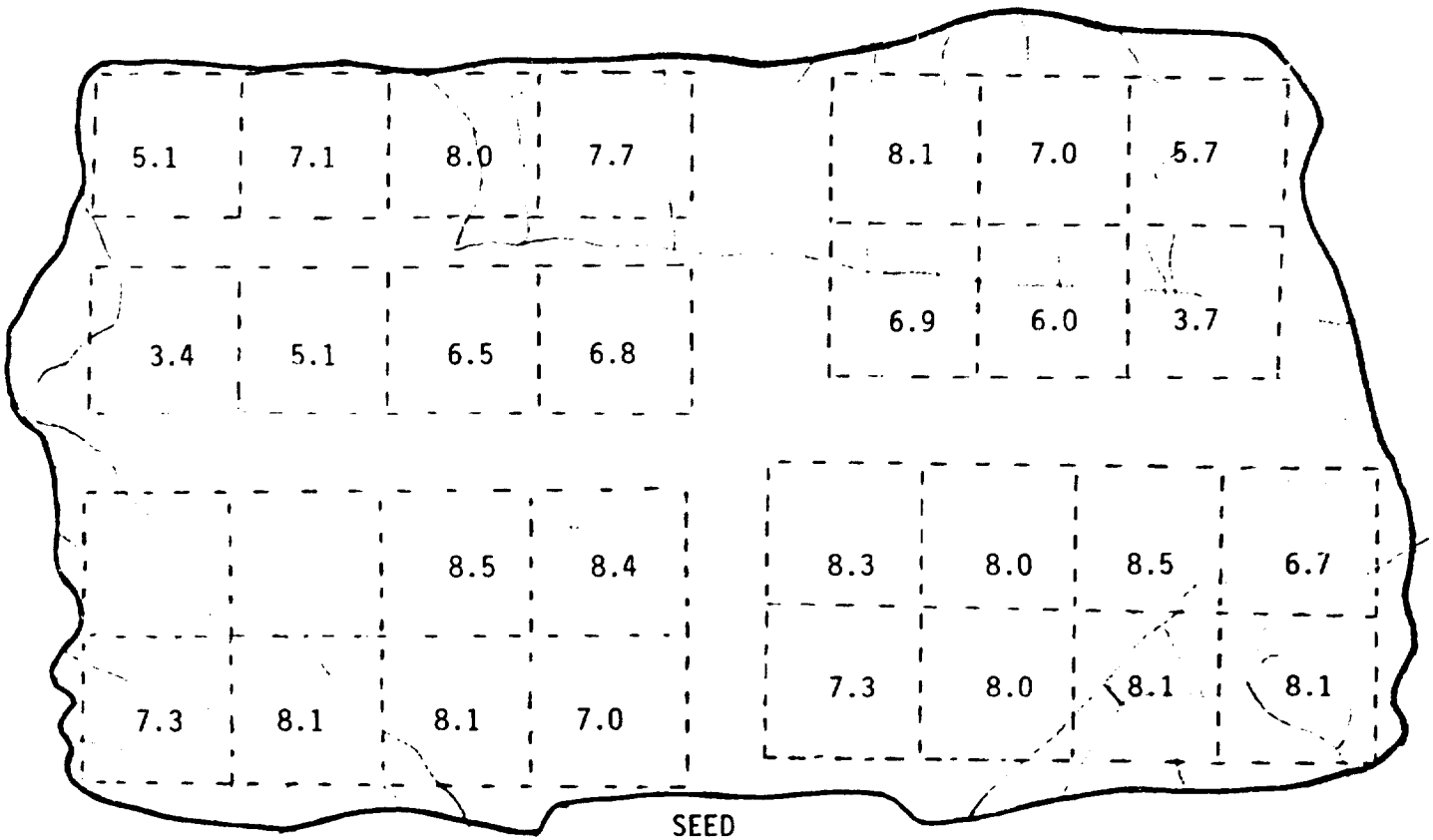

NOTE: UNIT: %

η OF CONTROL CELL = 9.1

FIGURE 18

EFFICIENCY (NORMALIZED WRT TO THE CONTROL CELLS) MAPPING OF A VERTICALLY CUT HEM WAFER FROM A CAST INGOT (#41-24)

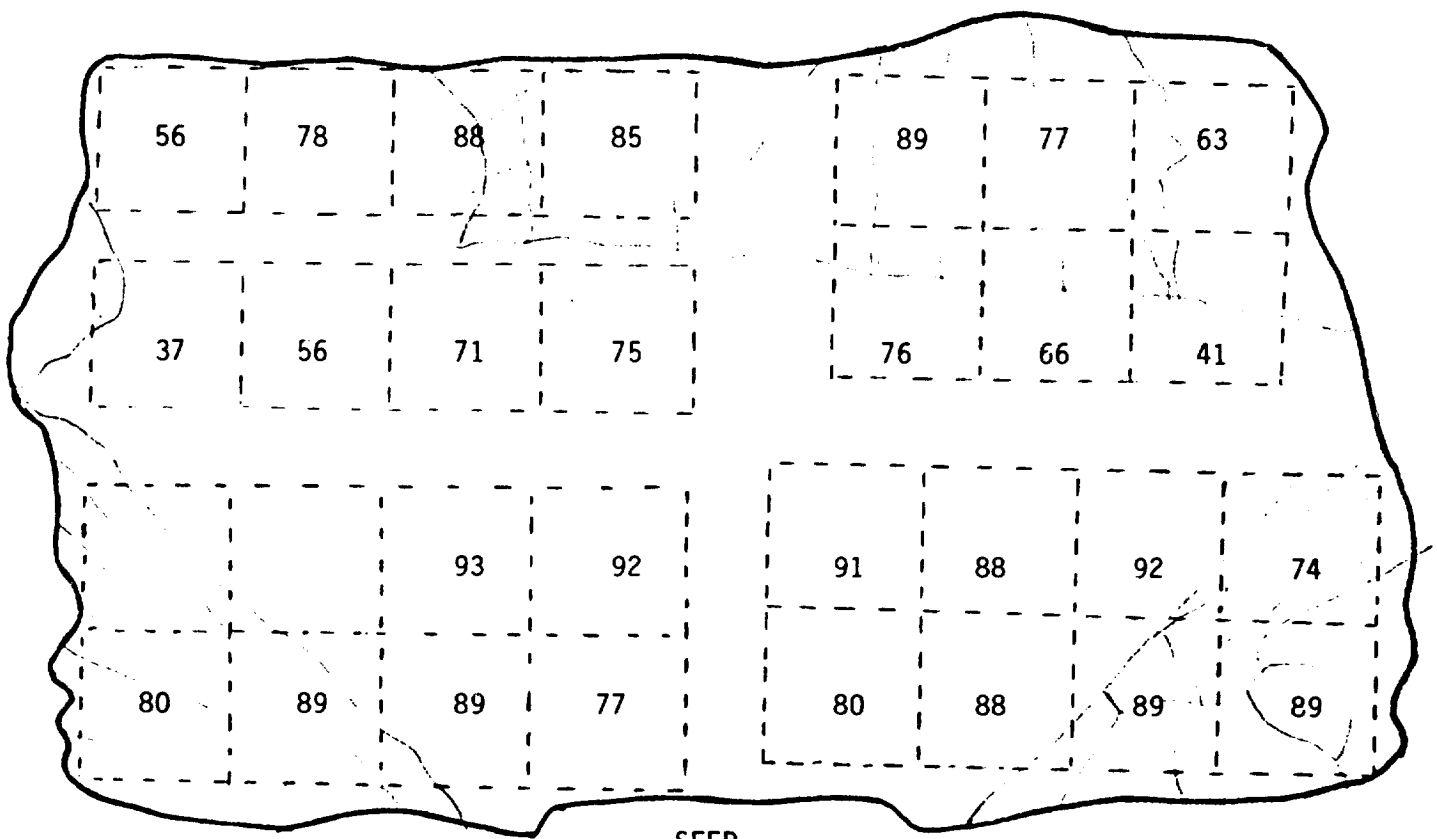

NOTE: UNIT: Percentage

AVERAGE: 78

FIGURE 19

EFFICIENCY (NORMALIZED WRT THE CZ CONTROL CELLS) MAPPING OF VERTICALLY CUT HEM (#41-24) BASELINE CELLS WITH THE GETTERING STEPS ADDED

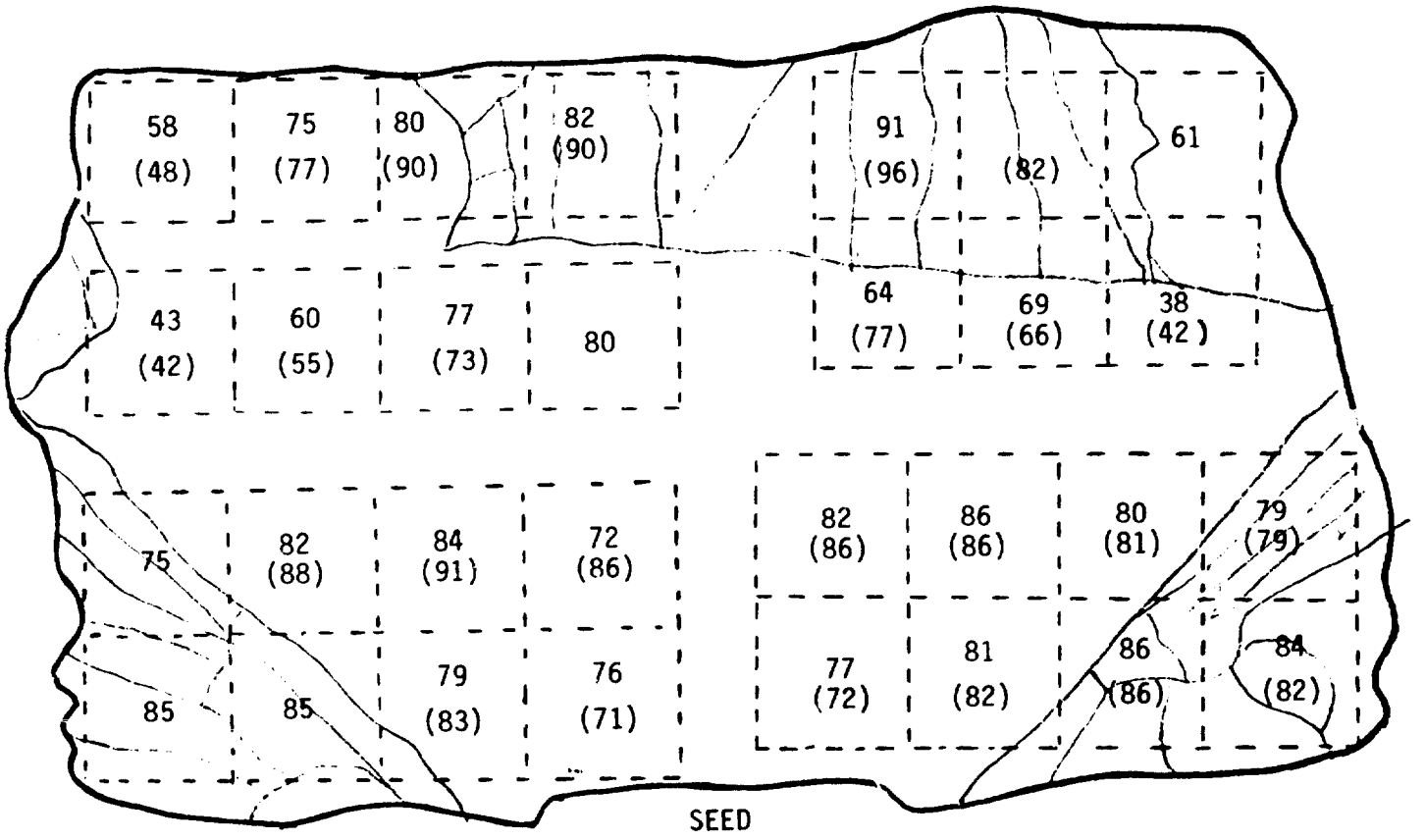

NOTE: 1) Unit: Percentage

2) Parenthesis numbers for the cells with the gettering step done after the chemical polishing.

FIGURE 20

L_D vs. No. of Suns for Vertically Cut HEM (#41-24) Cells
(Cells' No. in Parenthesis)

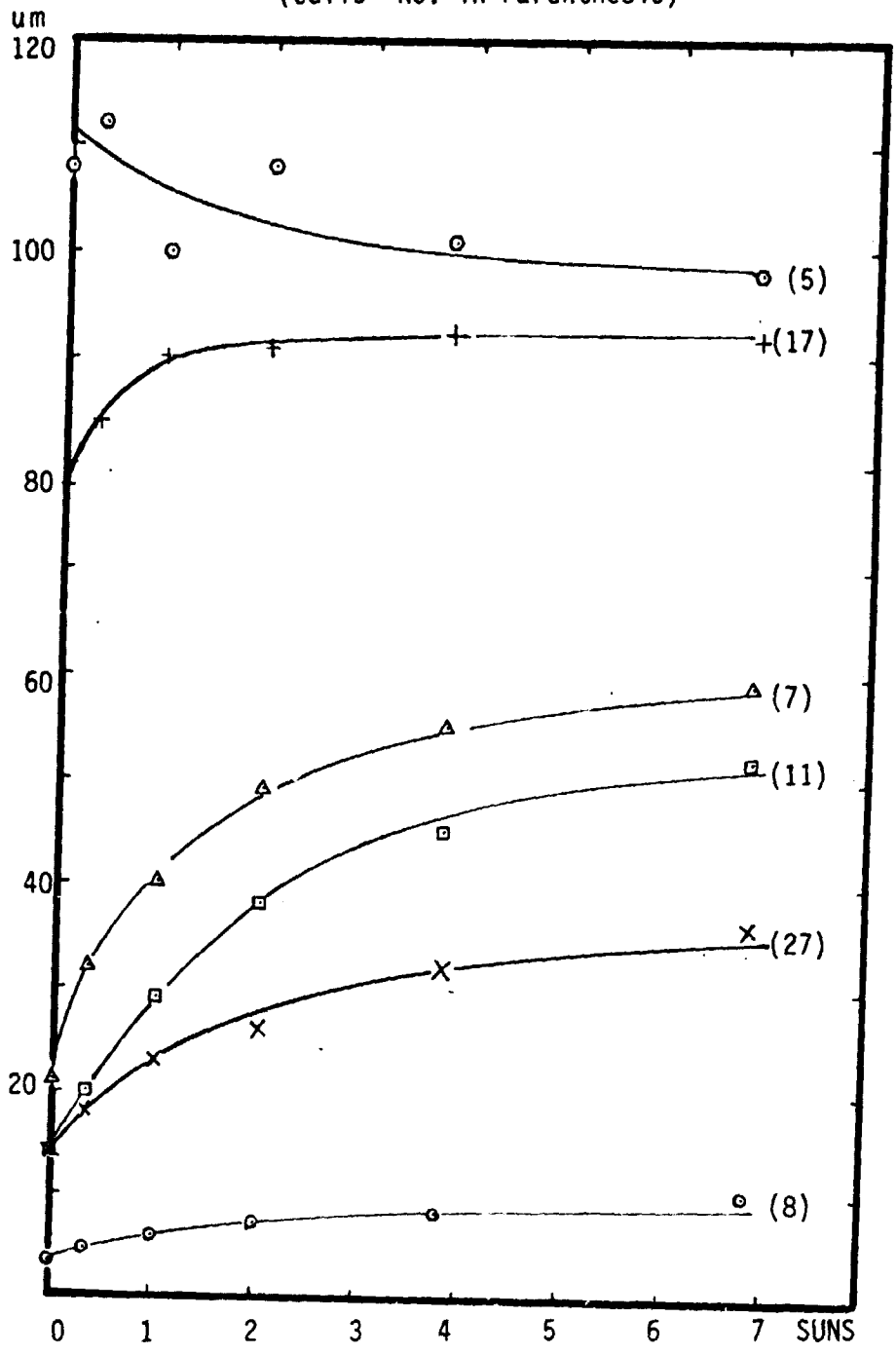

3.0 Solar Cells From A Large Cast Ingot (#41-41C)

Solar Cell Fabrication

Baseline solar cells were fabricated on wafers cut from a large cast ingot (ingot #41-41C was 12"x 12"x 6" in dimension, ~40kg). The positions where the wafers were cut is illustrated in Figure 21. Cross section layers of half ingots were cut at three vertical positions and three horizontal positions for each ingot. About 48 - 2x2cm cells were fabricated on each layer chosen to represent each ingot position. Cell fabrication was completed in all six layers for the ingot. Resistivity measured by four point probe was about 2 ohm-cm with p-type conductivity.

Characteristics Under Illumination

Finished baseline solar cells had SiO AR coating and about 90% active area with Ti-Pd-Ag metallization. Solar cell parameters, such as Isc, Voc, CFF, and n were measured under AM1 conditions at 28°C test block temperature. Figures 22 to Figure 27 show the mappings of cells normalized n (to CZ control) on all six layers for the ingot. This ingot demonstrated the best performance for all the HEM ingots measured to date. Except for the region close to the seed at center bottom, with some areas showing low Jsc and shunting problems (top layer), the cell performances were quite uniform throughout the ingot including the polycrystalline area. (See the Figures in text.) The overall efficiency of the usable area of the ingot is about 87% of that of the baseline CZ control cells.

Spectral Response

Absolute spectral response (A/W) measurements were made using a filter wheel set-up. Response versus wavelength of selected cells from a center layer

is given in Figure 28. The figure shows a variation of the response (mostly in long wavelength region) from cell to cell depending on the position.

Minority Carrier Diffusion Length

Minority carrier diffusion length (L_D) was measured on the same solar cells used to measure spectral response, using the short circuit current method. The results of spectral response and minority carrier diffusion length measurements indicate that there is substantial variation of L_D from top to bottom in the ingots (from 15um to 120um, mostly above 30um). This variation is not reflected as strongly from the Jsc data because Jsc does not drop substantially until L_D 40um. However, one would expect that more pronounced differences will show up when a back surface field is added.

FIGURE 21

WAFER IDENTIFICATION WITHIN THE LARGE HEM INGOT

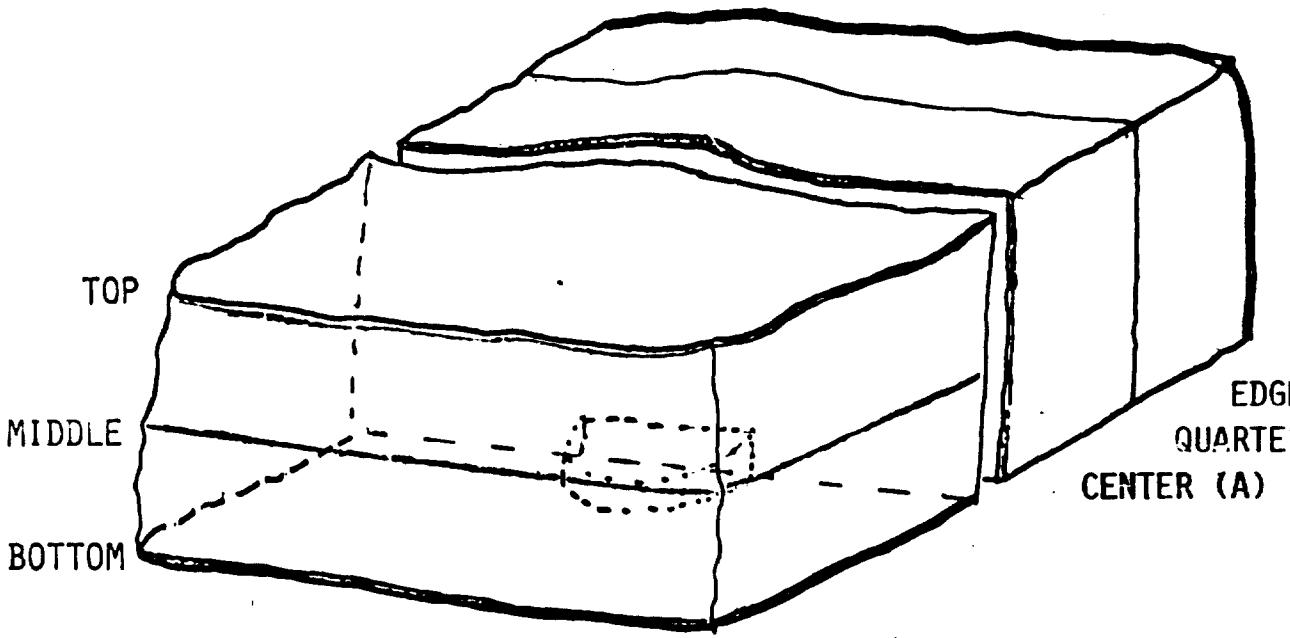

SIZE: 12" x 12" x 6"

WT. ~ 35 kg

FIGURE 22

A MAPPING OF NORMALIZED η (% TO CONTROL) FOR A CENTER LAYER OF VERTICALLY CUT HEM (41-41C)

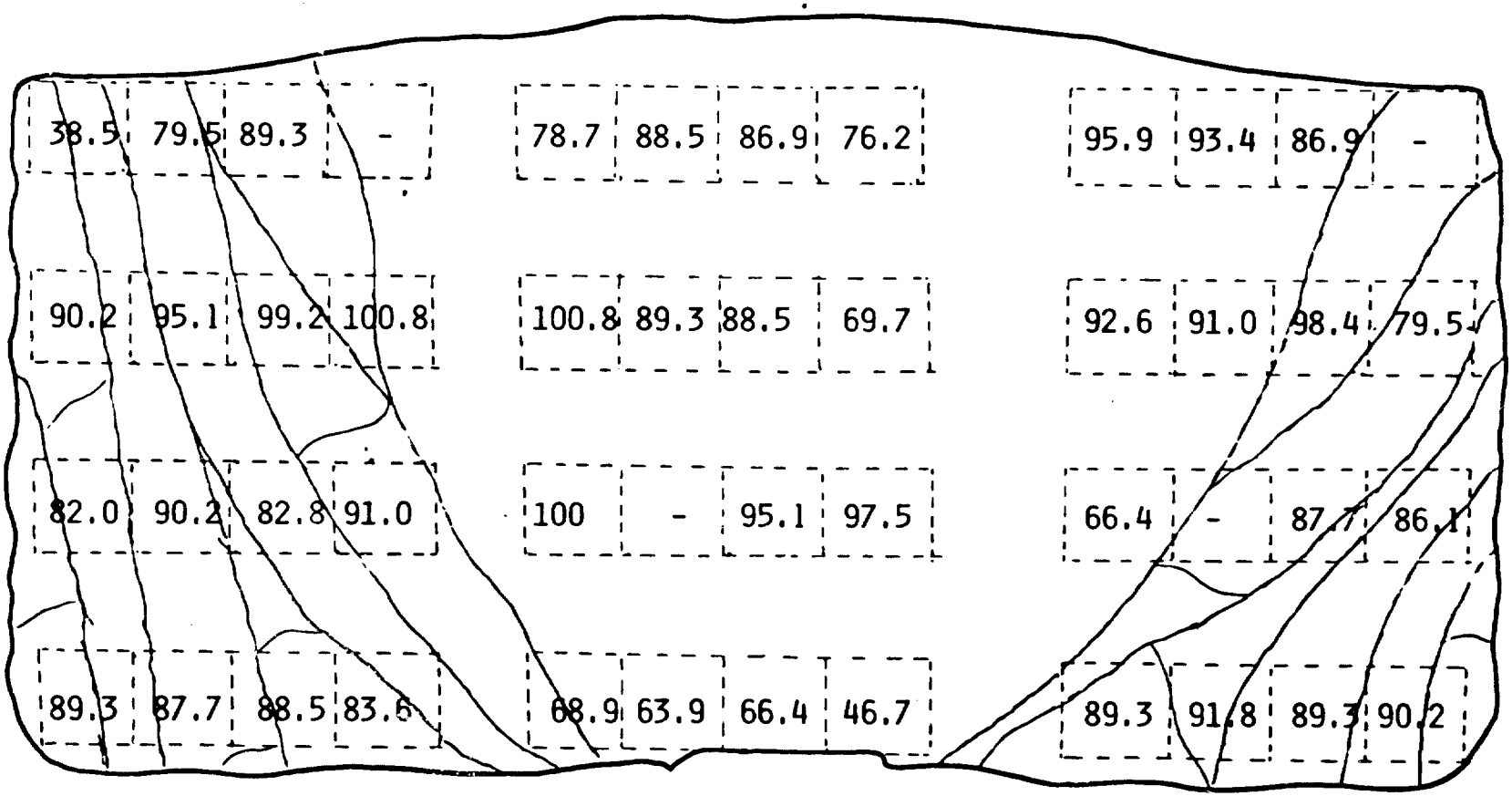

AVE. 85.1%

FIGURE 23

A MAPPING OF NORMALIZED η (% TO CONTROL) FOR A QUARTER LAYER OF VERTICALLY CUT HEM (41-41C)

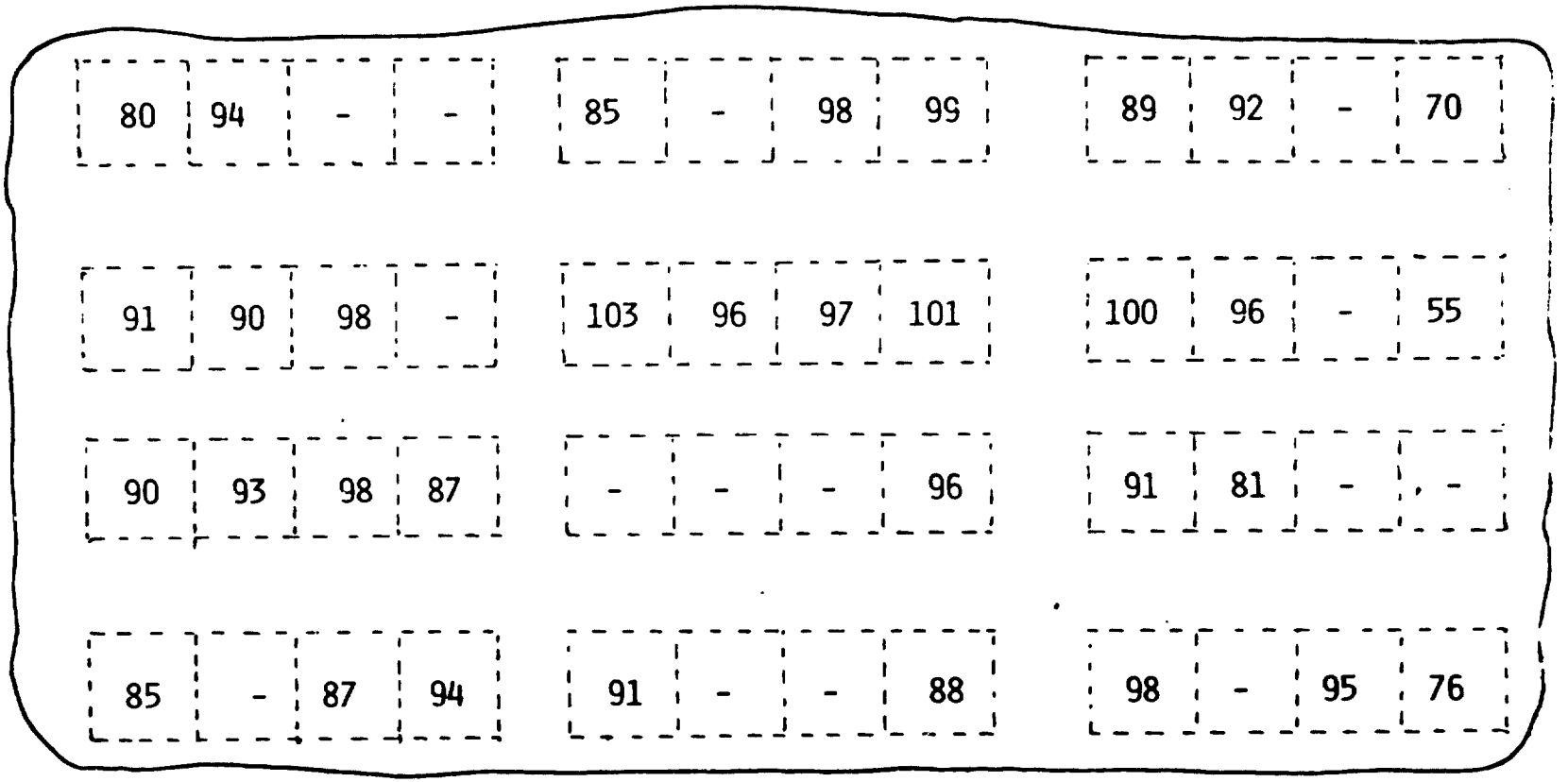

AVE. 90%

FIGURE 24

A MAPPING OF NORMALIZED η (% TO CONTROL) FOR A EDGE LAYER OF VERTICALLY CUT HEM (41-41C)

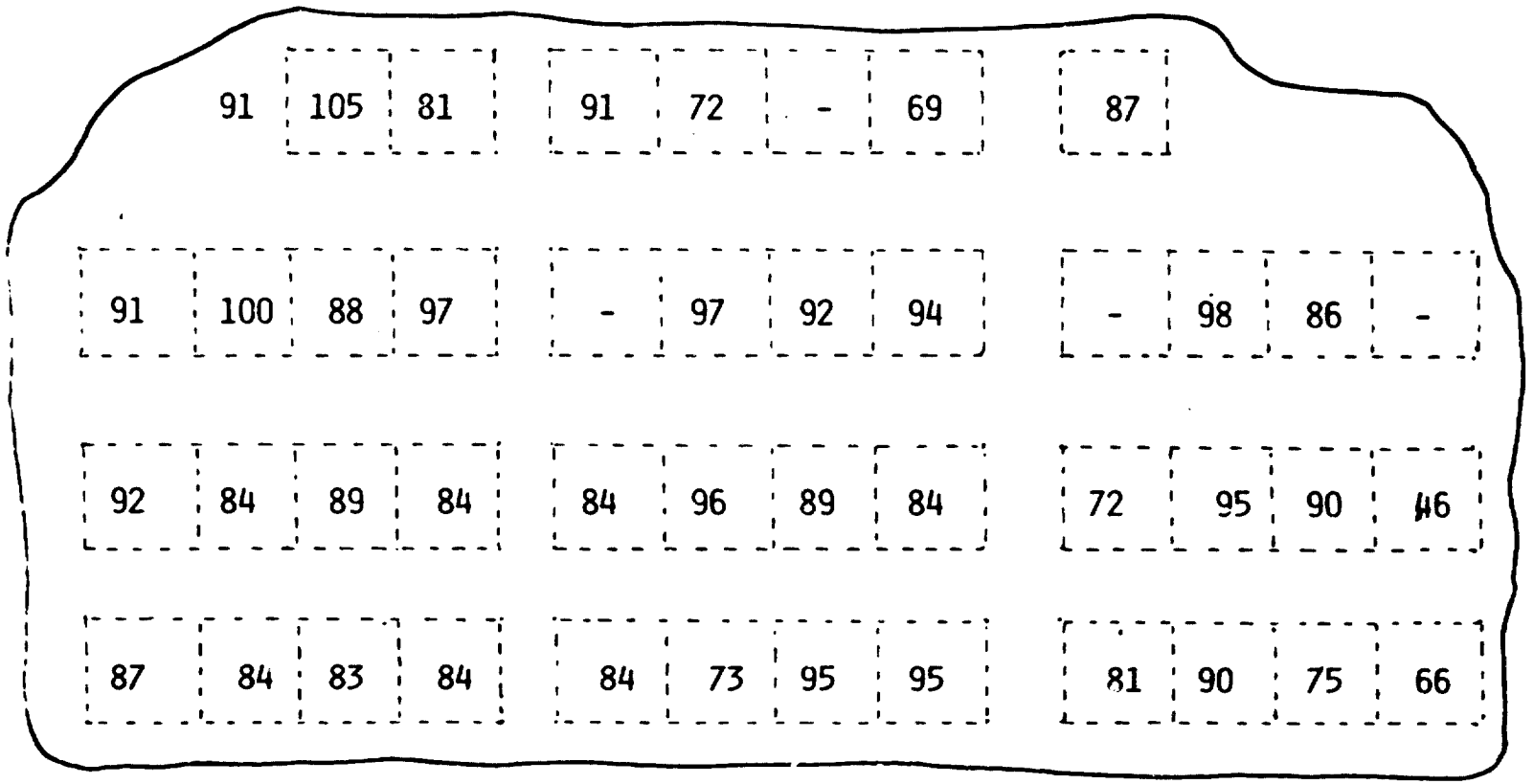

AVE. 86%

FIGURE 25

A MAPPING OF NORMALIZED7/ (% TO CONTROL) FOR THE TOP HORIZONTAL LAYER OF HEM (41-41C)

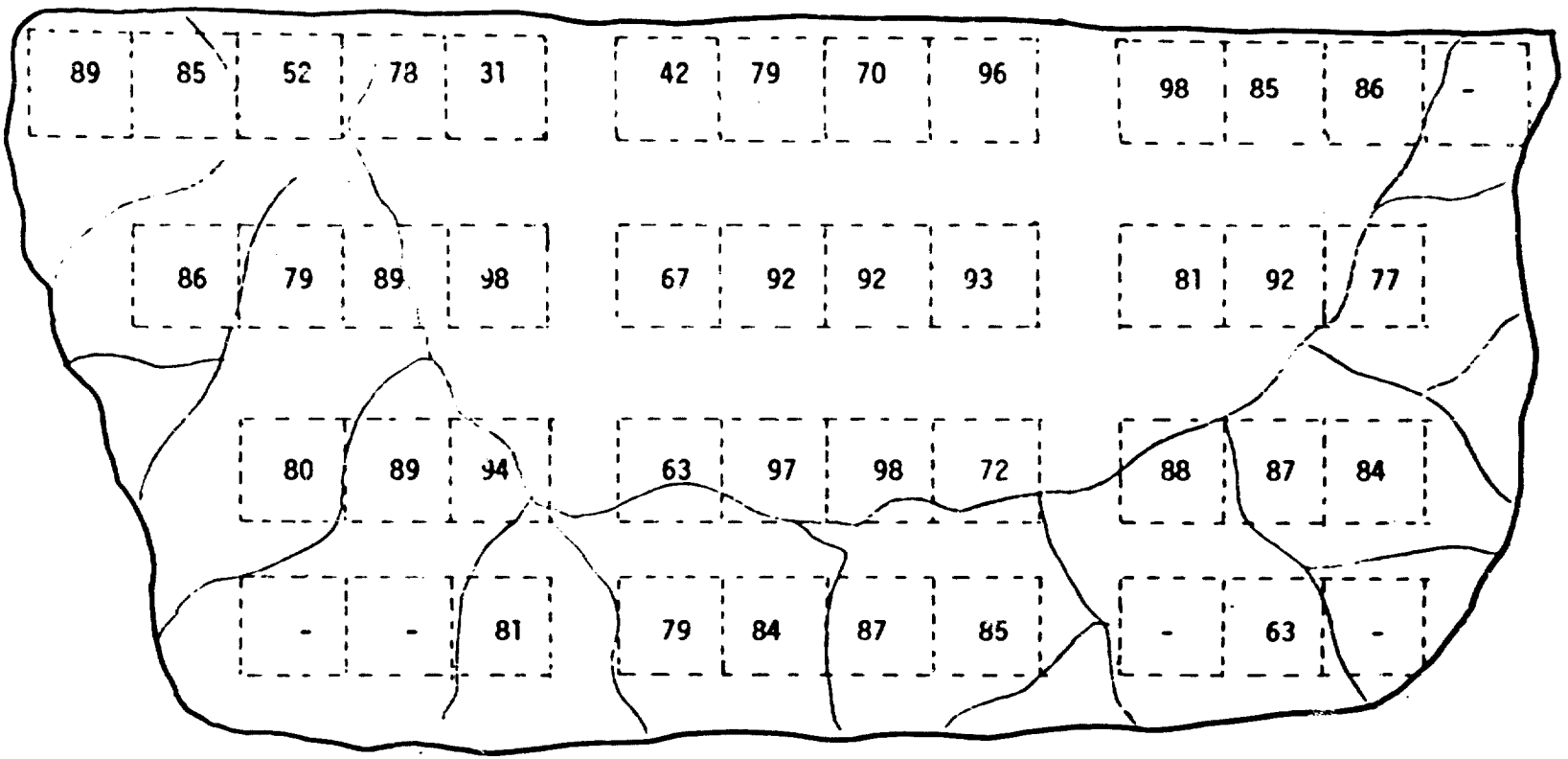

AVE. 82%

FIGURE 26

A MAPPING OF NORMALIZED η (% TO CONTROL) FOR THE MIDDLE HORIZONTAL LAYER OF HEM (41-41C)

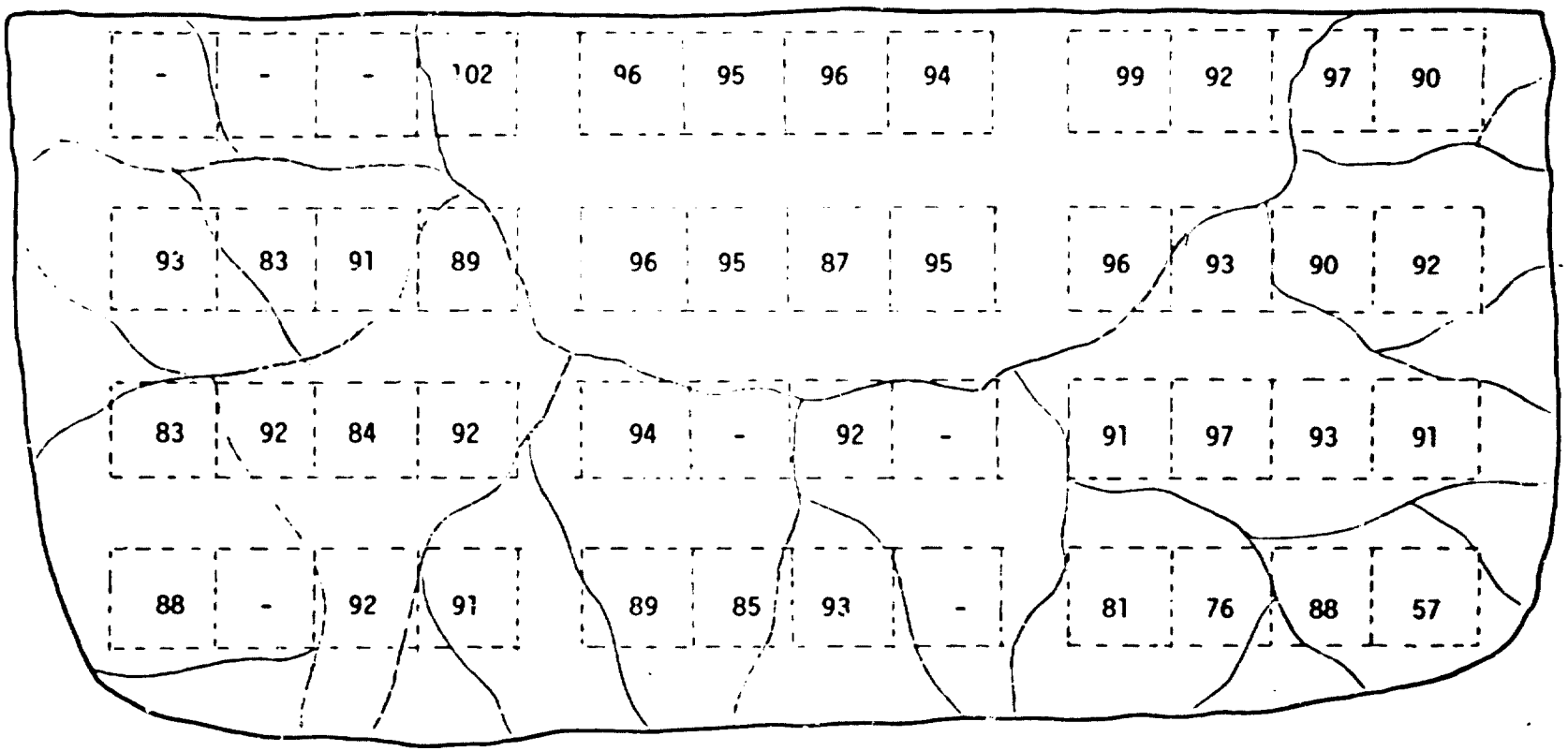

AVE. 90%

FIGURE 27

A MAPPING OF NORMALIZED η (% TO CONTROL) FOR THE BOTTOM HORIZONTAL LAYER OF HEM (41-41C)

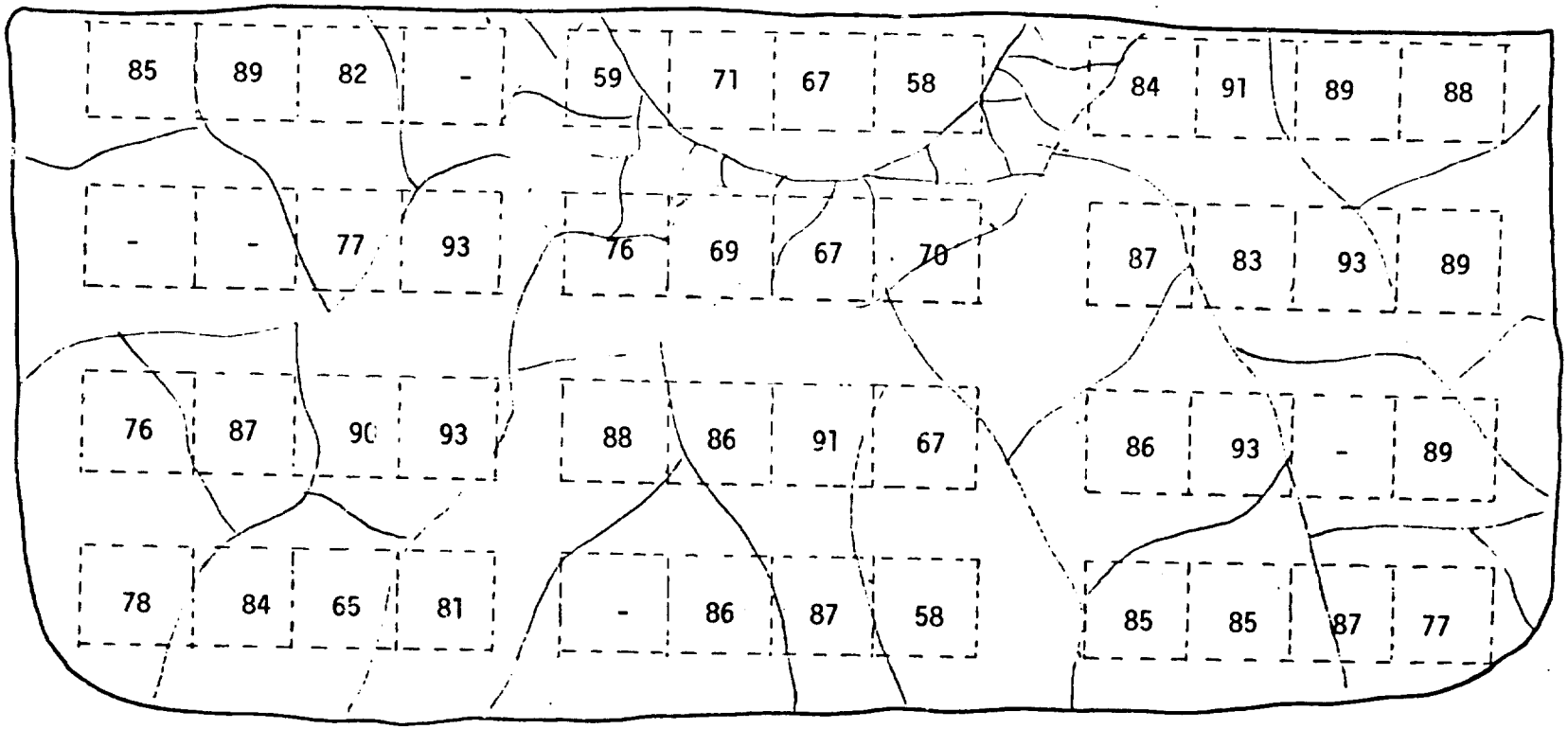

AVE. 81%

FIGURE 28A

SPECTRAL RESPONSES OF SELECTED SAMPLES FROM A CENTER LAYER OF VERTICALLY CUT HEM(41-41C)

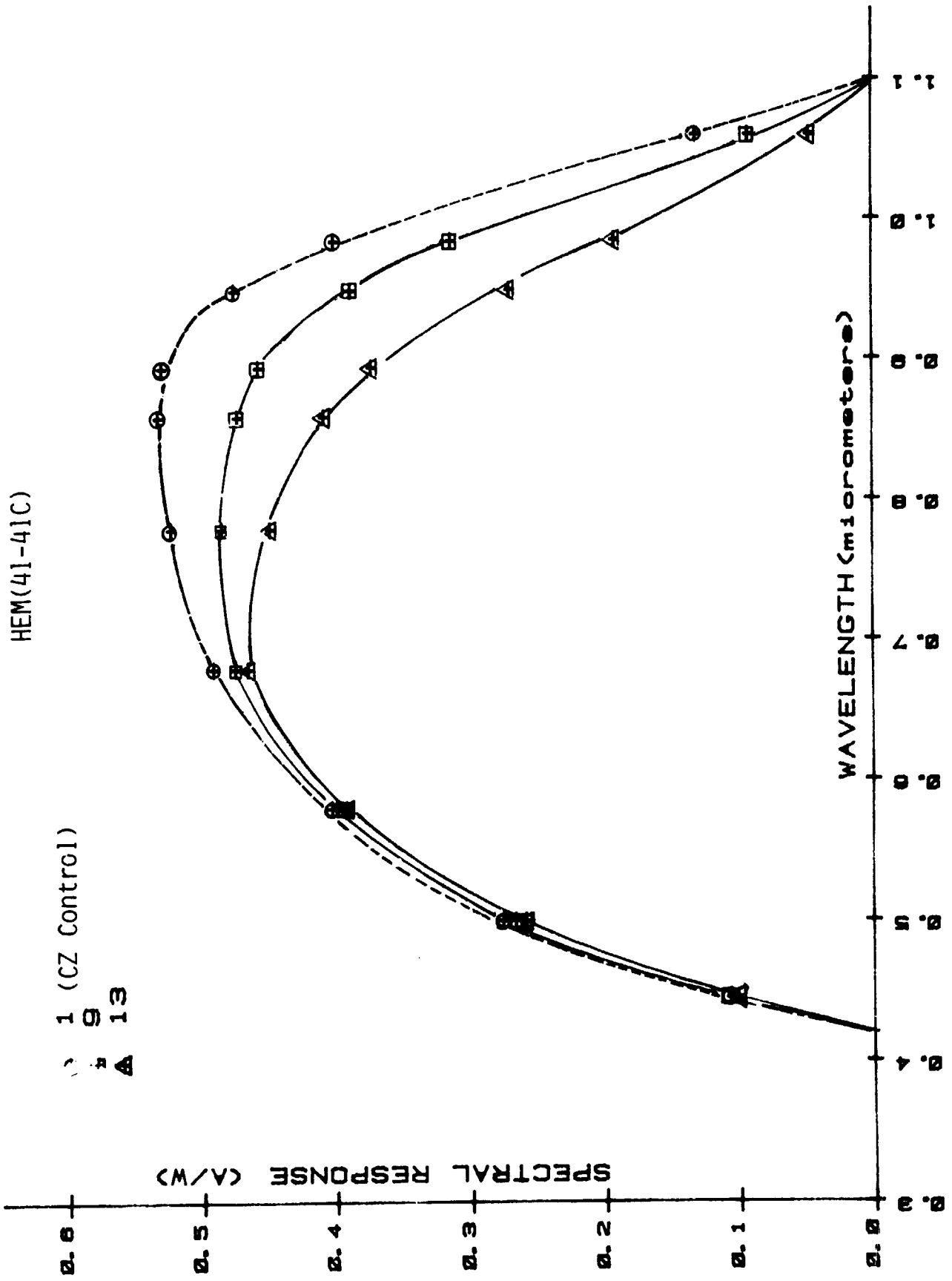

FIGURE 28B

SPECTRAL RESPONSES OF SELECTED SAMPLE FROM A CENTER LAYER OF VERTICALLY CUT HEM (41-41C)

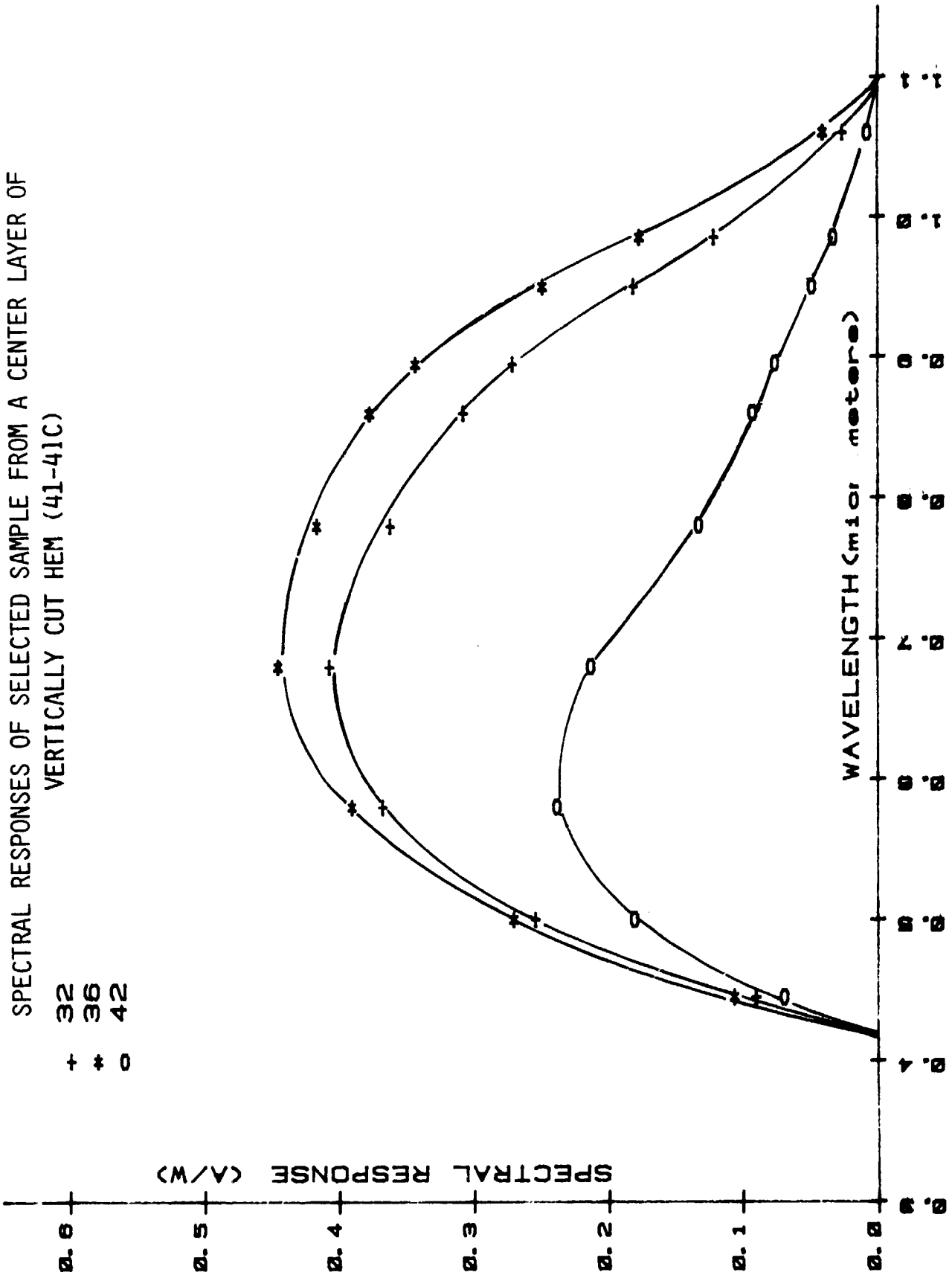

4.0 Solar Cells From A Large Cast Ingot (#41-48)

Solar Cell Fabrication

Methods like those described in section 3.0 were used for the evaluation of another large cast ingot (12"x 12"x 6", 40kg). Measured resistivity was about 6 ohm-cm with P-type conductivity.

Characteristics Under Illumination

Baseline solar cells had about 90% active area with SiO AR coating. Solar cell parameters such as Voc, Jsc, CFF, and n were obtained under AM1 simulation conditions at 28°C test block temperature.

Figure 29 to Figure 31 show mappings of normalized n (to CZ control) of cells for each of the three vertically cut layers and Figures 32 to Figure 34 show results of the three horizontally cut layers. The solar cell performance of this ingot is much worse than that of #41-41C. Voc and CFF indicated severe shunting problems in relatively large portions of the ingot, especially close to the edge. (The shunted areas are separated out in the figures and excluded from the averaging of efficiency). The cause of the shunting is not immediately known. Portions of the shunting area had high density of micro-precipitates as shown in the microscope pictures of Figure 35. In some cases these micro-precipitates were observed at grain boundaries of very fine grain areas. However, these fine grain areas only account for a small portion of the total shunting area. Inclusions were also noted in some other areas in the bulk.

The shunted area is estimated to be about 30 to 35% of the whole ingot, mostly occurring along the edge and on the top of the upper half of the ingot (see figures). The top polycrystalline area where the final solidification occurred

seems to be shunted m st as judged by the cell performance. Other areas showing shunting problems are polycrystalline areas along the edge downward. The single crystalline area and the lower polycrystalline areas away from the edge are relatively free of the shunting problems. It could be speculated that the shunting is caused by inclusions, most likely precipitates at the final solidification stage. These results merit further material study. The total effectiveness of the ingot was estimated to be about 60% compared to a CZ control ingot.

Spectral Response

Absolute spectral response (A/W) measurements were made using a filter wheel set-up. Response of the selected cells from a vertically cut center layer is shown in Figure 36, indicating poor performance of some cells in the long wavelength region.

Minority Carrier Diffusion Length

Minority carrier diffusion length (L_D) was measured on the finished solar cells using the short circuit current method. Measurements gave similar results with the ingot (#41-41C) in previous section, showing a wide variation of L_D from 10 to 110um depending on the location.

FIGURE 29

A MAPPING OF NORMALIZED η (% TO CONTROL) FOR A CENTER LAYER OF VERTICALLY CUT HEM (41-48)

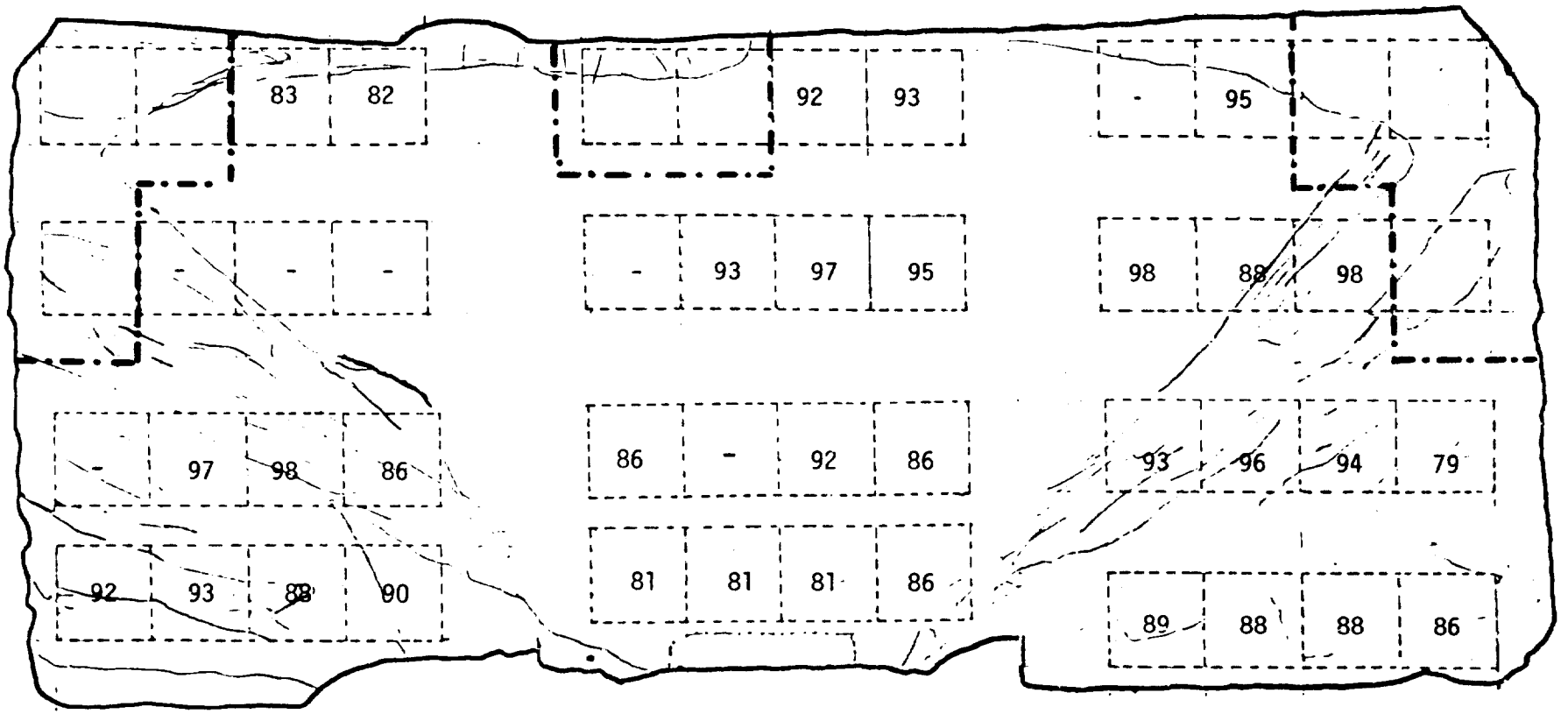

AVE. OF USABLE AREA: 90 (Regions separated by —·— lines are excluded due to shunting.)

FIGURE 30

A MAPPING OF NORMALIZED η (% TO CONTROL) FOR A QUARTER LAYER OF VERTICALLY CUT HEM (41-48)

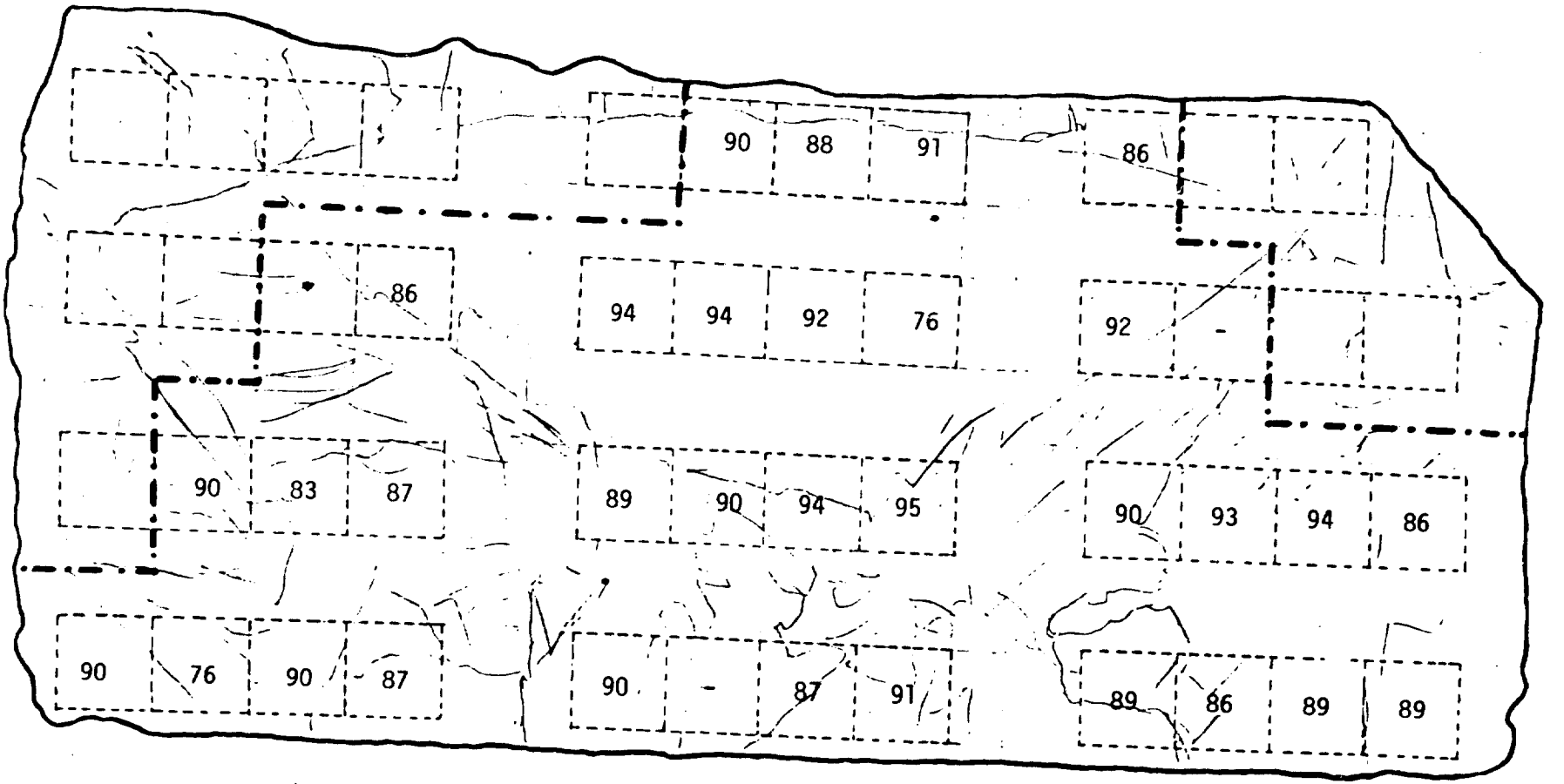

AVE. OF USABLE AREA: 89% (Regions separated by -·- lines are excluded due to shunting.)

FIGURE 31

A MAPPING OF NORMALIZED η (% TO CONTROL) FOR A EDGE LAYER OF VERTICALLY CUT HEM (41-48)

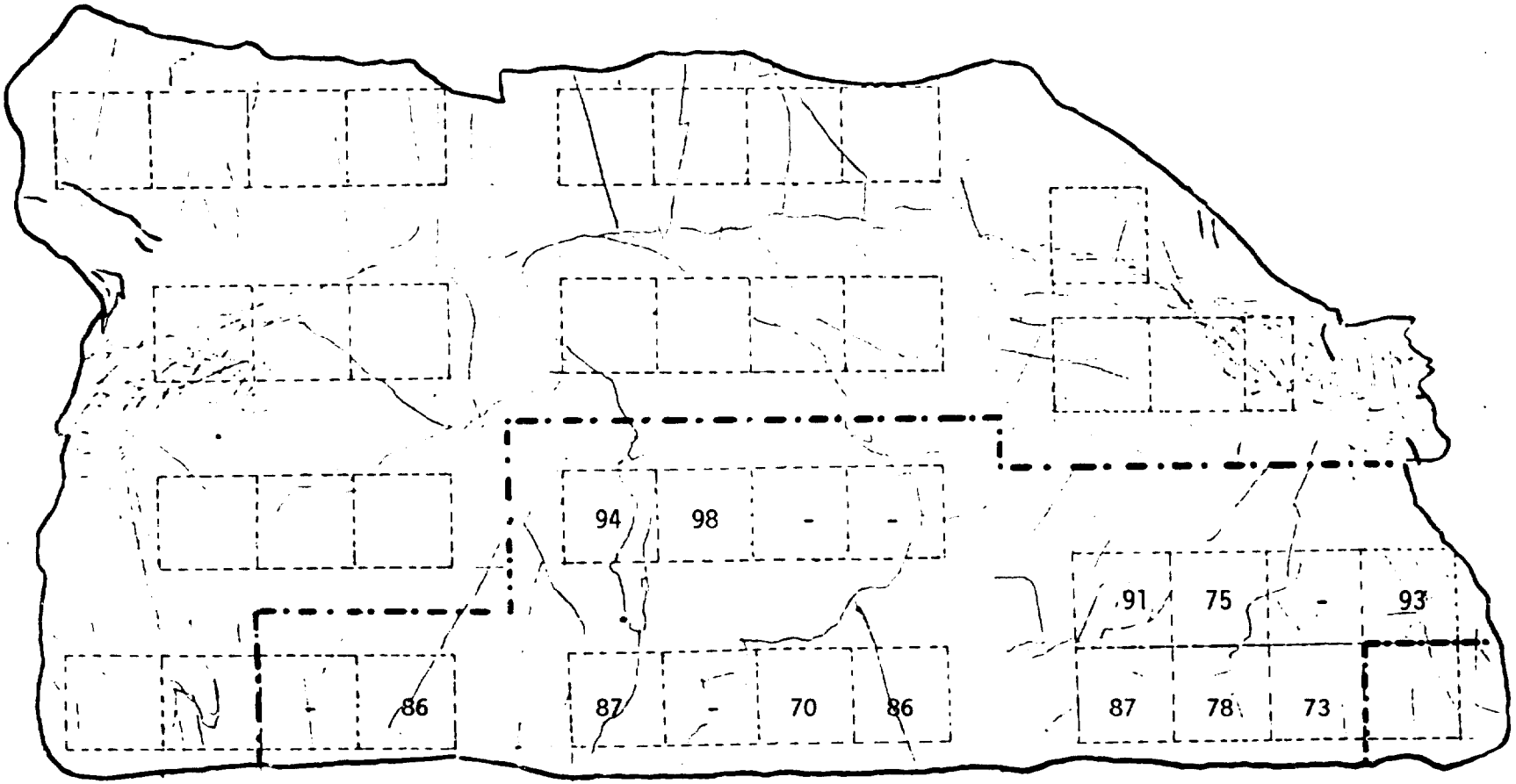

AVE. OF USABLE AREA: 84% (Regions seaprated by —·— lines are excluded due to shunting. In this case, the whole upper region is excluded.)

FIGURE 32

A MAPPING OF NORMALIZED η (% TO CONTROL) OF A TOP LAYER OF HORIZONTALLY CUT HEM(41-48)

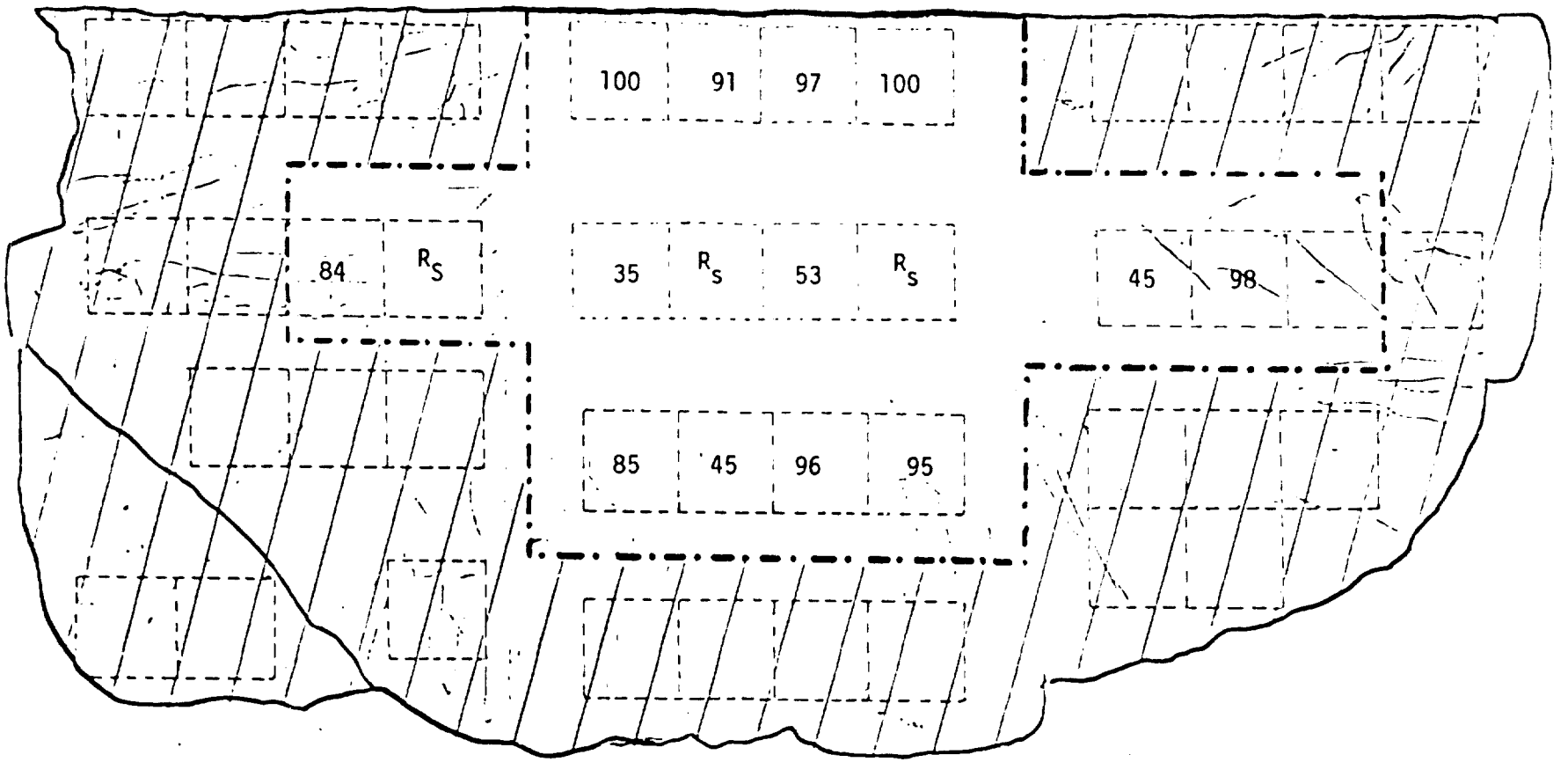

AVE. OF USABLE AREA: 79% (SHADED AREAS ///ARE EXCLUDED DUE TO SHUNTI

ESTIMATED PERCENTAGE OF USABLE AREA: 39%

ESTIMATED TOTAL EFFICIENCY VS. CONTROL: .79 x .39 = 31%

FIGURE 33

A MAPPING OF NORMALIZED η (% TO CONTROL) OF A MIDDLE LAYER OF HORIZONTALLY CUT(HEM 41-48)

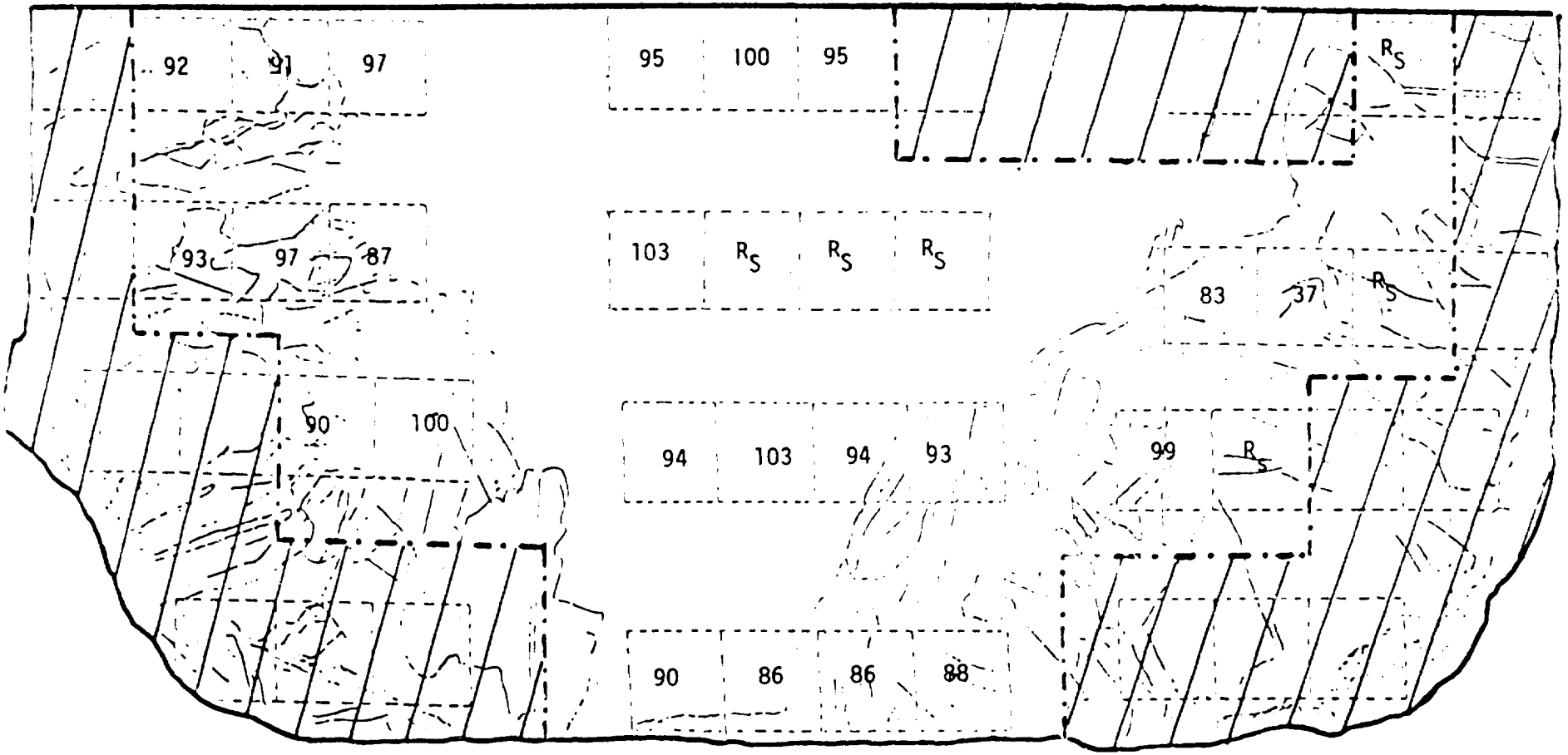

AVE. OF USABLE AREA: 91% (SHADED AREA ARE EXCLUDED DUE TO SHUNTING)

ESTIMATED PERCENTAGE OF USABLE (i.e. NON-SHADED) AREA: 67%

TOTAL EFFICIENCY VS. CONTROL: .91 x .67% = 61%

FIGURE 34

A MAPPING OF NORMALIZED η (% TO CONTROL) OF A BOTTOM LAYER OF HORIZONTALLY CUT(HEM 41-48)

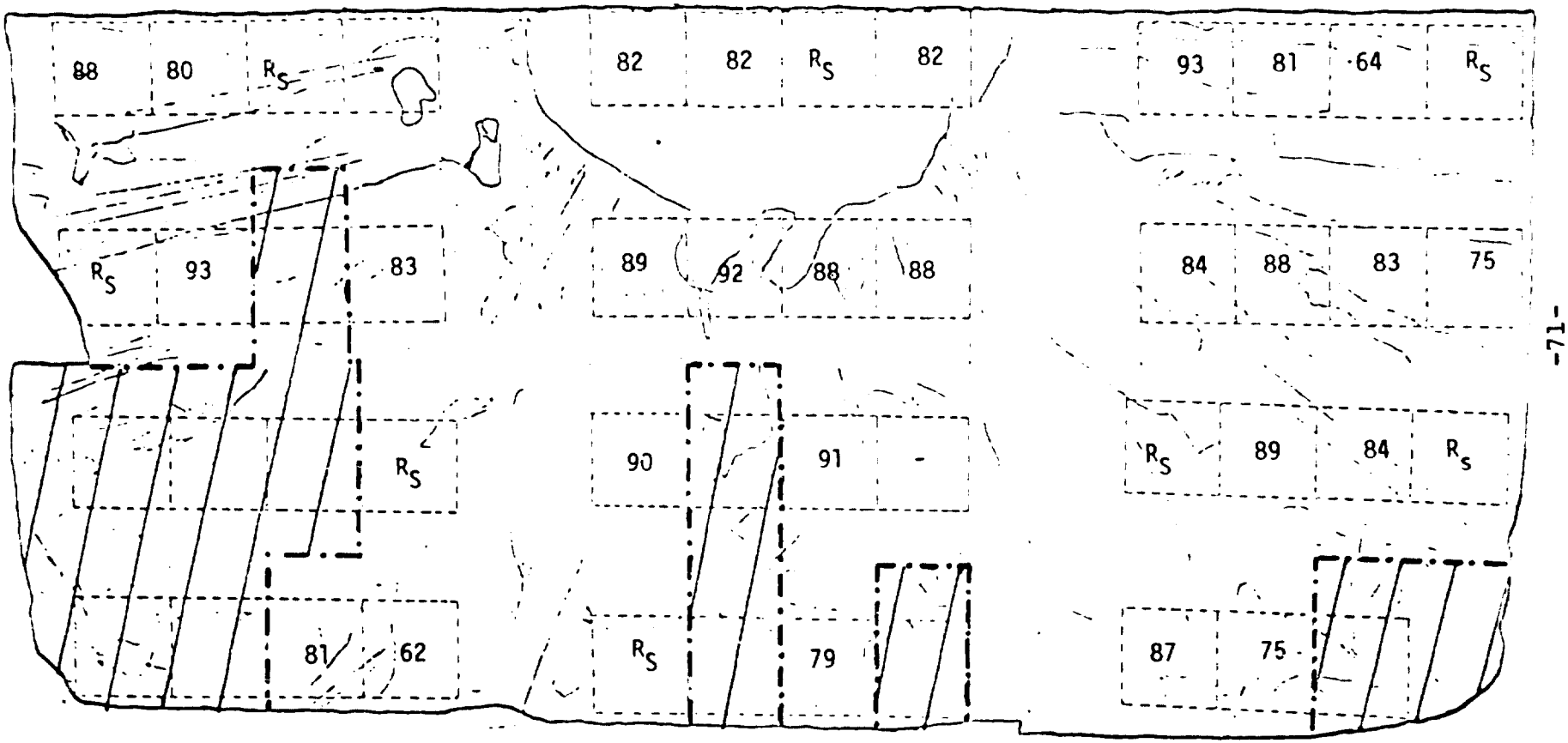

AVE. OF USABLE AREA: 83% (SHADED AREA///ARE EXCLUDED DUE TO SHUNTING)
ESTIMATED PERCENTAGE OF USABLE (i.e. NONSHADED) AREA: 89%
ESTIMATED TOTAL EFFICIENCY VS. CONTROL: .83 x .89 = 74%

FIGURE 35

Microscopic Picture of Inclusions Observed in a HEM Ingot (41-48), 200X Magnification

FIGURE 36

SPECTRAL RESPONSES OF SELECTED SAMPLES OF A CENTER LAYER OF VERTICALLY CUT HEM (41-48)

D. Solar Cells From Cast Ingot By Ubiquitous Crystallization Process (UCP)

1.0 Solar Cell Fabrication

Six (6) polycrystalline UCP wafers (10x10cm) representating six (6) different groups of material were delivered. Each wafer was polished and cut to 2x2cm blanks with their position marked (see Figure 37 for the positions). With the orientation of each wafer and its position in each group of material known, one can use the results of the cell performance to correlate with the properties of each material group.

All wafers were polycrystalline with mm size grains. Measured resistivity was about 3 ohm-cm. Baseline process was applied to fabricate solar cells. Refer to reference (9) for the details of UCP process.

2.0 Solar Cell Performance and Characterization

Characteristics Under Illumination

Solar cell parameters, such as Jsc, Voc, CFF, and n were measured under AM1 conditions at 28°C test block temperature. The results of the cells are summarized in Table 15. One can see from the Table that the cell performance was relatively uniform. The few cells which had shunting problems showed inclusions under microscope observation. Figure 38 shows microscopic pictures of the inclusions observed in a cell which showed severe shunting problems.

Analysis of data and visual observation indicated that the variation of Jsc was related to the grain size of the material and the average Jsc was lower than the CZ control by more than 11%. The lower Voc could be partly accounted for by slightly higher resistivity of the material (~3ohm-cm) than the CZ control (~1 ohm-cm). The average efficiency was considerably lower than the CZ control; 10.6% versus 13.1%.

Spectral Response

Absolute spectral response (A/W) was measured using the filter wheel set-up. Plots of the response of representative cells without AR coating are given in Figure 39. The UCP cells gave lower response than the CZ control cell, especially at long wavelength (> 0.6um), suggesting reduced minority carrier diffusion length.

Minority Carrier Diffusion Length

Effective minority carrier diffusion length (L_D) was obtained using the short circuit current method of the finished solar cells. Results from selected samples are summarized in Table 16, in which short circuit current density information is given in right hand column for reference. The table indicates a range of L_D from 20 to 80um, with a typical L_D of around 40-50um.

Photoresponse By Small Light Spot Scanning

Localized photoresponse of the UCP solar cells was obtained by light scanning. Refer to Appendix of Reference (1) for the details of the measurement. Typical scanning results are given in Figure 40, in which (A) represents scanning of a cell which is relatively free from grain boundaries, and (B) response of a cell with small grain structure. The cell with smaller grains showed reduced response, and wide spectral variations. Photoresponse of the CZ control cells are shown.

The figures indicate that response in the bulk of the UCP cell is lower than the CZ controls.

FIGURE 37

MAPPING OF THE 2 X 2 CELLS IN SEMIX WAFER

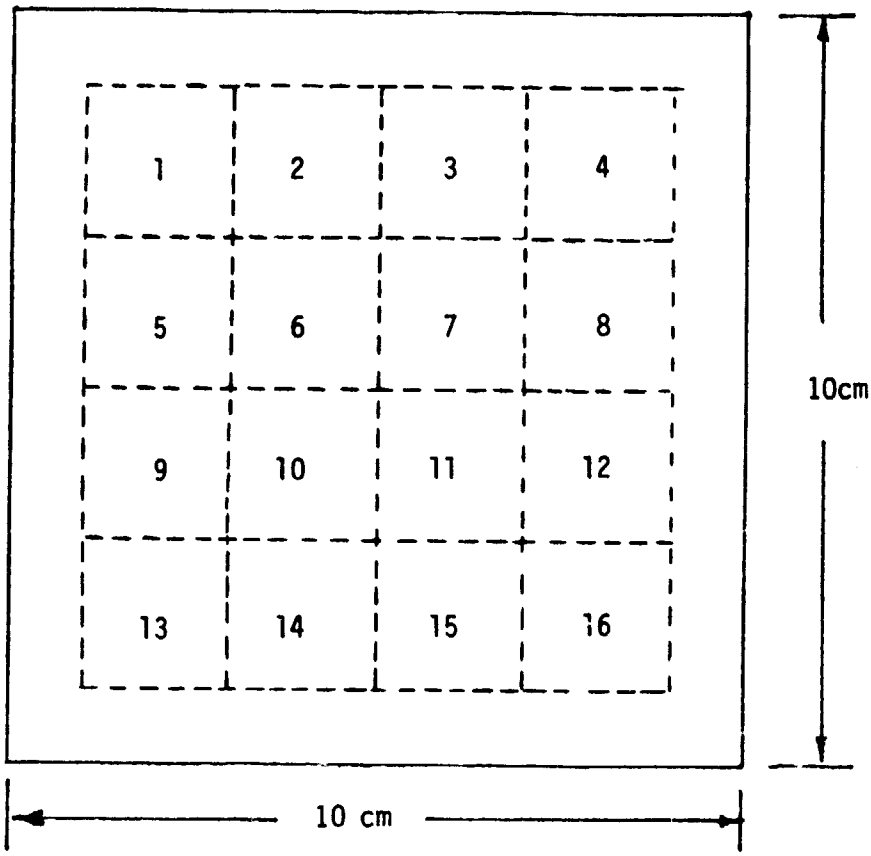

Shown here are the cells' number and their positions with the orientation of the wafer pre-determined.

(a)

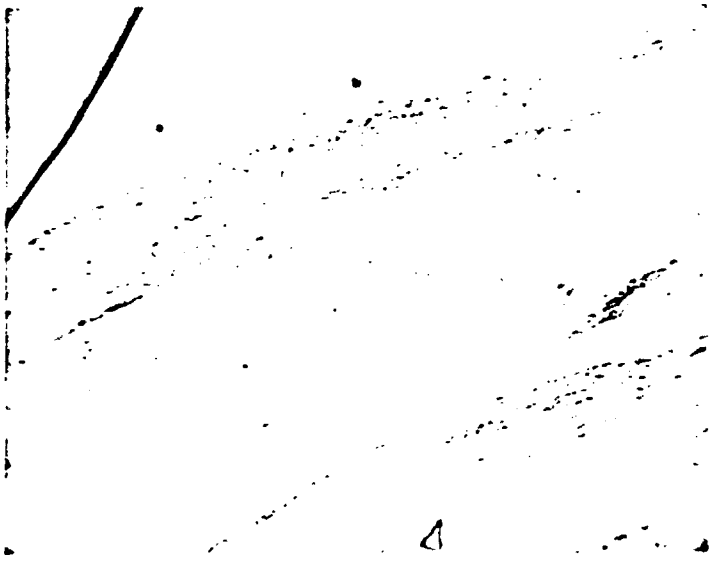

(b)

FIGURE 38. Microscopic Photographs of Inclusions (or Precipitates) Observed in UCP Wafers 200X Magnification, (a) From a Cell (#E-13), (b) From a Cell (#E5).

FIGURE 39. SPECTRAL RESPONSE OF BASELINE SOLAR CELLS (NO AR) FROM UCP

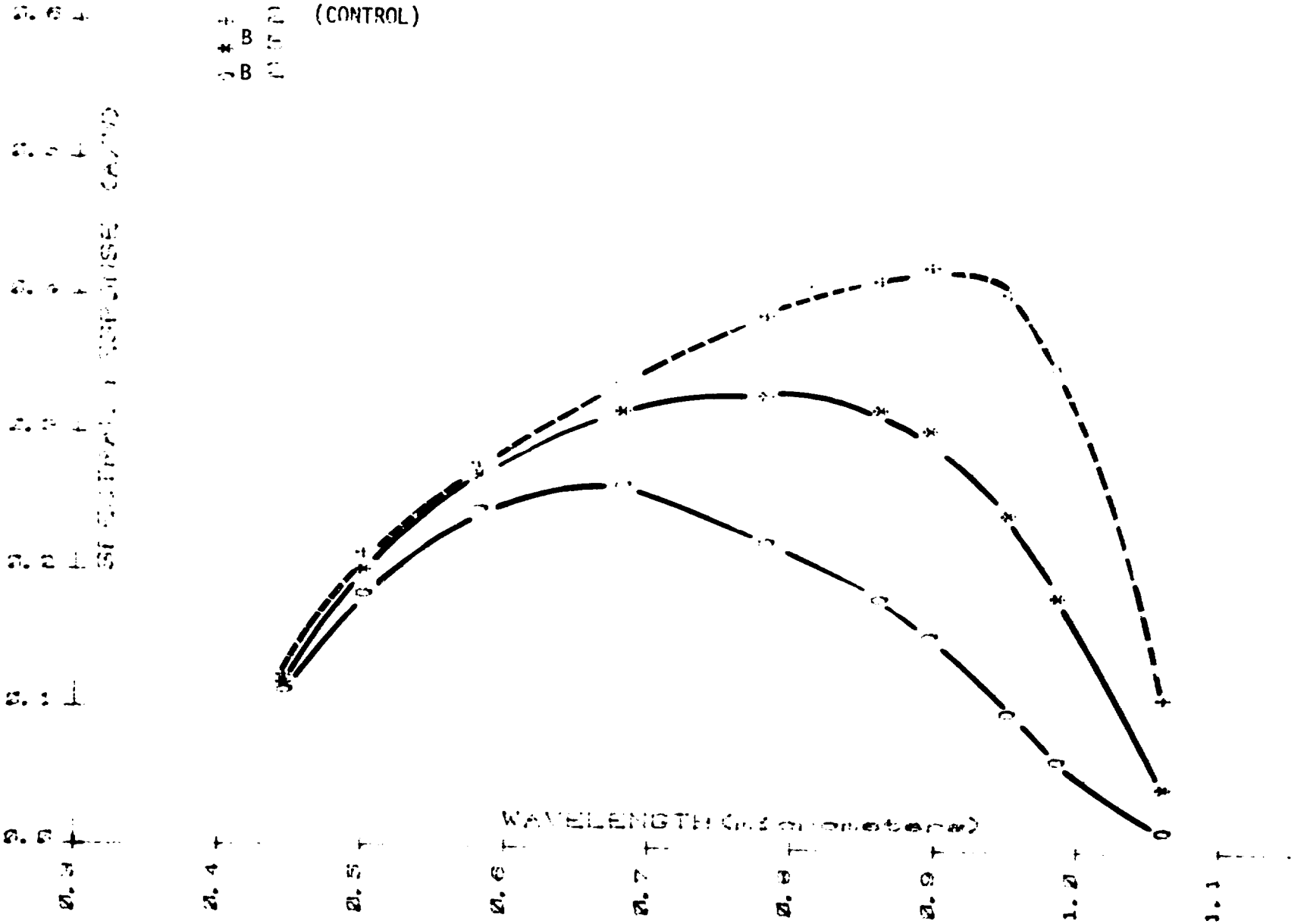

FIGURE 40(A)

SMALL LIGHT SPOT SCANNING OF A BASELINE CELL FROM UCP

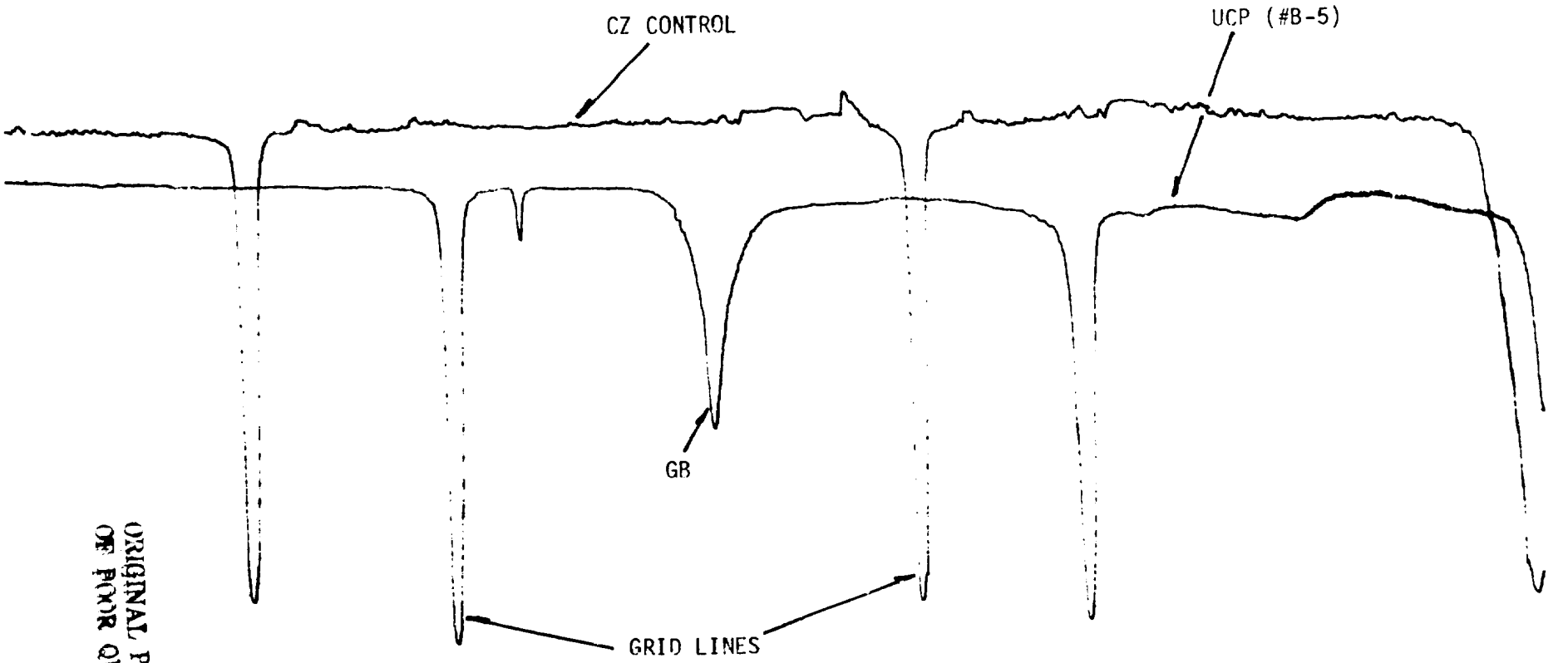

FIGURE 40 (B) CONTINUED

SMALL LIGHT SPOT SCANNING OF A BASELINE CELL FROM UCP

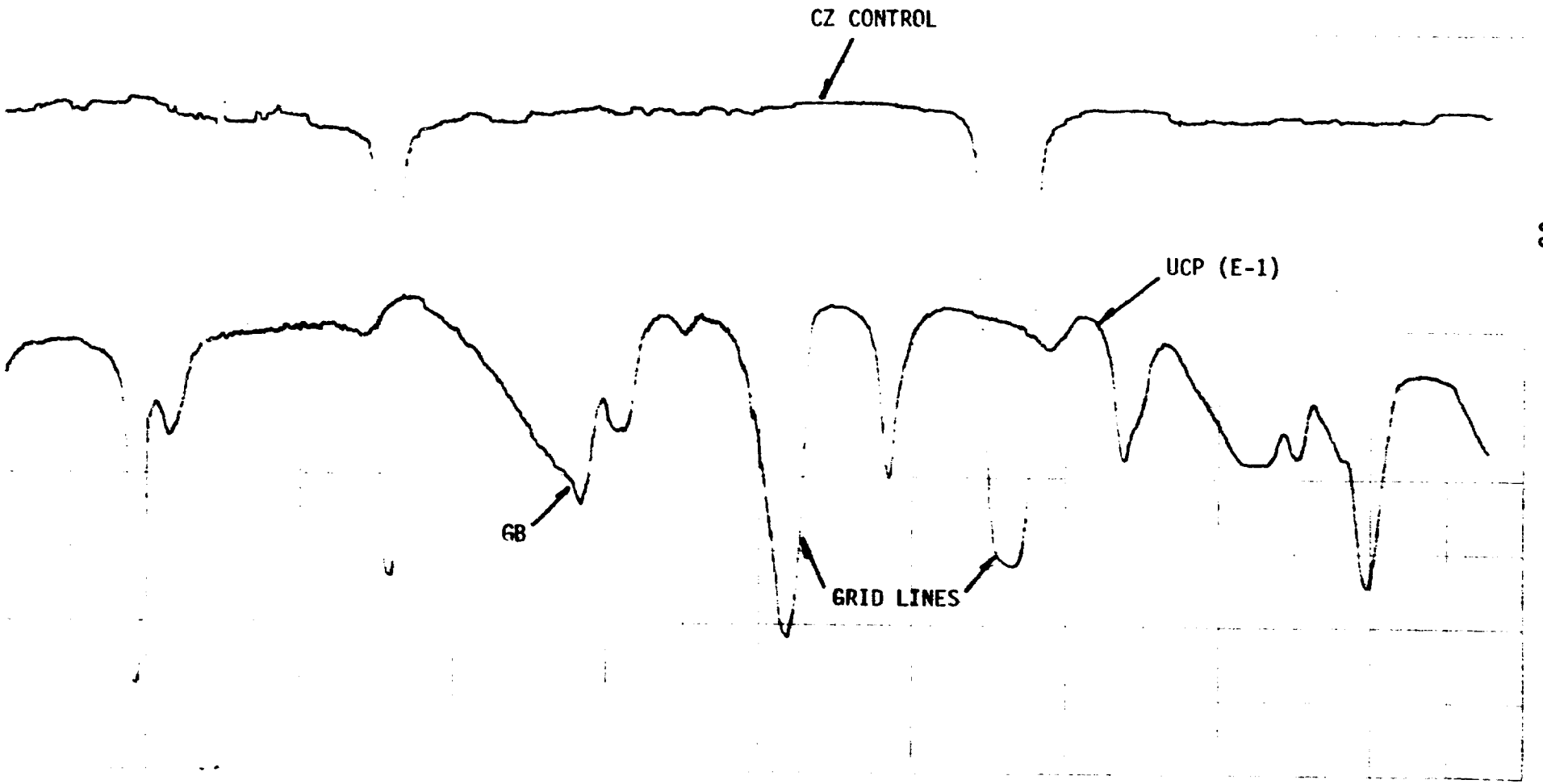

TABLE 15

SUMMARY OF RESULTS OF THE SOLAR CELLS FROM CAST INGOT BY UCP

WAFER #		Voc (mV)	Jsc (mA/cm^2)	CFF (%)	η (%)	NO.OF CELLS
A-5	Ave. S.D. Range	559 6 546-570	25.1 0.9 23.0-26.4	78 1 74-79	10.9 0.5 9.9-11.8	14
B-3	Ave. S.D. Range	554 9 540-568	25.1 1.2 23.1-26.9	76 2 70-79	10.6 0.7 9.6-12.0	15
C-1	Ave. S.D. Range	550 5 542-558	25.5 0.5 24.4-26.4	76 1 73-77	10.7 0.4 9.7-11.1	12
D-3	Ave. S.D. Range	557 8 542-568	26.0 0.7 25.0-26.8	76 2 70-78	11.0 .6 9.5-11.7	12
E-7	Ave. S.D. Range	543 14 504-558	25.4 0.6 24.0-26.1	72 10 44-78	9.9 1.5 5.5-11.2	12
F-3	Ave. S.D. Range	555 7 540-570	24.9 0.8 23.1-26.1	75 2 72-78	10.4 0.5 9.4-11.5	13
Combining All Wafers	Ave. Range	553 504-570	25.3 23.0-26.9	76 44-79	10.6 5.5-12.0	7[illegible]
CZ Control	Ave. S.D. Range	586 - -	28.7 0.2 28.5-28.9	78 1 77-79	13.1 0.1 13.0-13.2	3

TABLE 16

EFFECTIVE MINORITY CARRIER DIFFUSION LENGTH OF SOLAR CELLS

MADE FROM UCP WAFERS

	CELL NO.	L_D(um)	Jsc(mA/cm^2) (No AR)
GOOD CELLS	A-5-10	48	18.6
	B-3-5	72	19.2
	D-3-1	63	18.7
AVE.CELLS	A-5-15	44	17.6
	C-1-14	48	17.6
	E-7-1	46	17.6
BAD CELLS	A-5-12	28	16.3
	B-3-2	23	16.2
	F-3-6	37	16.3
	CONTROL #2	177	20.5

III. CONCLUSIONS AND RECOMMENDATIONS

The conclusions and recommendations reached after processing and evaluation of the sheets are as follows:

EFG Ribbons

- EFG ribbons grown in carbon containing gas atmosphere showed significant improvement in sheet quality. Chemical etching study indicated that new EFG showed better structural perfection; i.e., larger grain size and less dislocation density, and the diffusion length was significantly higher.

- The new EFG demonstrated an average baseline cell efficiency of 10.3% AM1 as opposed to 8.0% AM1 for the earlier EFG. The best efficiency achieved by the advanced process was 13.8% under AM1 conditions.

Dendritic Web

- Baseline solar cells from dendritic webs of various runs suggested that quality of the webs studied in this period was not as good as the conventional CZ silicon, about 60um versus 120um, and was slightly lower than that of the better web samples tested earlier.

- Performances of the baseline solar cells agree well with the dislocation counts analyzed by MRI, especially in terms of uniformity.

HEM

- Detail evaluation of four ingots suggested that HEM has problems of ingot reproducibility from run to run and also in uniformity of sheet quality within an ingot. Junction shunting was major cause of the problem, which could be due to the particulate inclusions observed in the bulk.

- Gettering and low temperature annealing experiment did not improve cell efficiency significantly. Detailed analysis of defects and impurities is necessary to identify the potential causes of degraded silicon sheet quality.

UCP

- Initial evaluation of the wafers prepared from the cast ingot by the process suggested that the quality of the wafers by this process is considerably lower than the CZ control; average baseline efficiency 10.6% versus 13.1%.

- Overall cell performance was relatively uniform with an exception of few cells which showed shunting problems caused by particulate inclusions.

IV. WORK PLAN STATUS

Next phase of the program is expected to continue efforts of the previous phases, with an emphasis on improvement of solar cell efficiency by process optimization and development of new techniques tailored to suit the specific sheet form. Efforts will be extended to fabricate larger area solar cells. Increased efforts will be made to correlate the results of defect studies at other laboratories, with the cell results.

V. REFERENCES

1. H.I. Yoo, et.al. "Silicon Solar Cell Process Development, Fabrication and Analysis". JPL Contract No. 955089, Annual Report (Phase I), June 1979.

2 H.I. Yoo, et.al. "Silicon Solar Cell Process Development, Fabrication and Analysis". JPL Contract No. 955089, Annual Report (Phase II), June 1980.

3. F.V. Wald, et.al. "Large Area Silicon Sheet by EFG", JPL Contract No. 954355, Technical Reports for the LSA Project, Mobil-Tyco.

4. F. Ferraris and F.C. Matacotta, "Optimized Diffusion Parameters for Cells Made byColumnar Silicon". Proc. of European Photovoltaic Solar Energy Conf., pp.625, October 1980.

5. R. Natesh, et.al. "Quantitative Analysis of Defects in Silicon". Final Report for the LSA Project, JPL, April 1980.

6. C.S. Duncan, et.al., "Silicon Web Process". JPL Contract No. 954654, Technical Report, Westinghouse.

7. F.Schmid, et.al., "Silicon Ingot Casting Heat Exchanger Method, Multi-Wire Slicing-Fixed Abrasive Slicing Technique". JPL Contract No. 954373, Technical Reports for the LSA Project, Crystal System.

8. D.V. Lange "Deep Level Transient Spectroscopy: A New Method to Characterize Traps in Semiconductors", Journal of Applied Physics, Vol.45, P.3023-3032, 1974.

9. "Semicrystalline Casting Process Development and Verification", SEMIX Inc., Technical Reports, DOE Contract No. DE-FC01-80ET-23199.

APPENDIX I

TIME SCHEDULE

TIME SCHEDULE

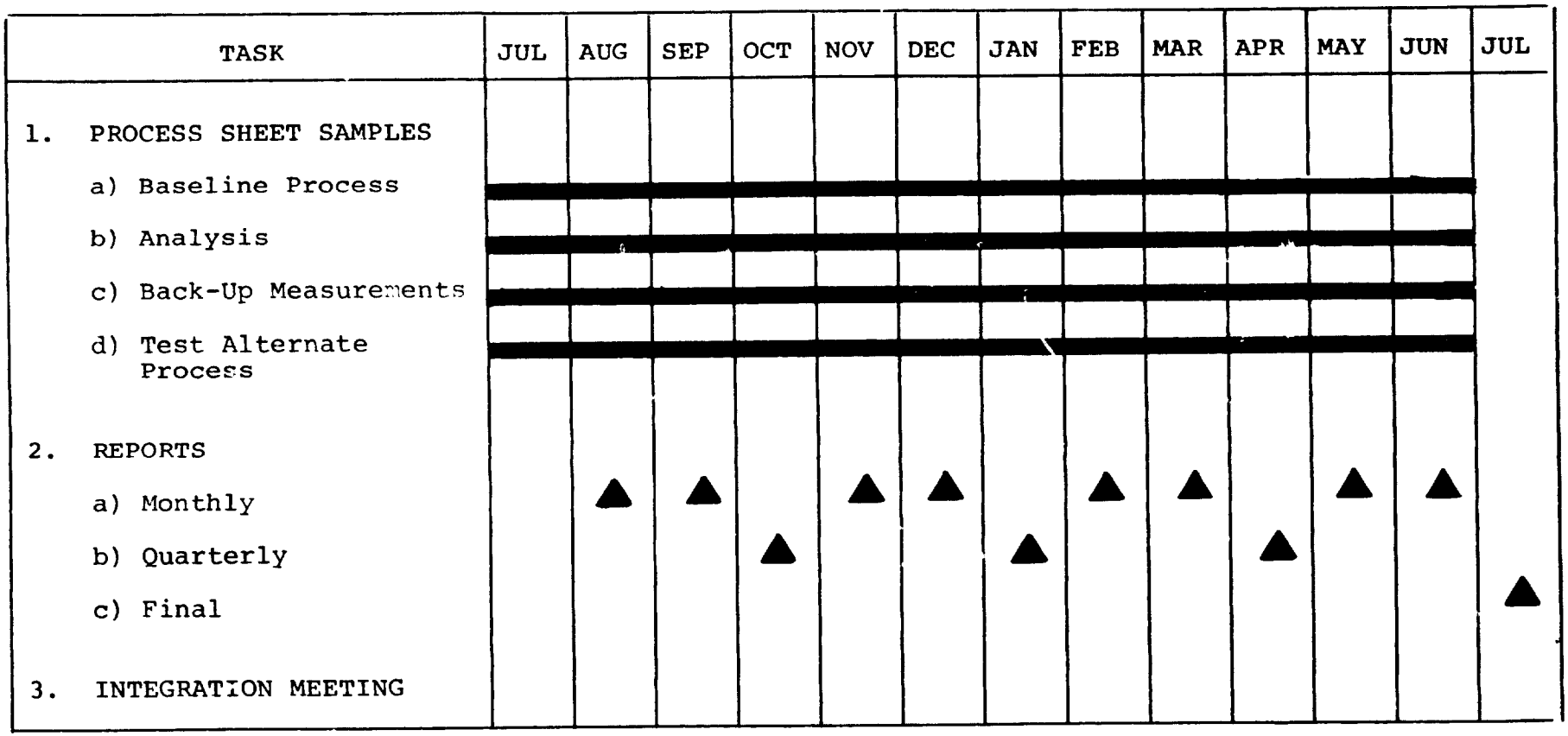

APPENDIX II

ABBREVIATIONS

V_{OC}:	Open Circuit Voltage
I_{SC}:	Short Circuit Current
J_{SC}:	Short Circuit Current Density
I_{SCR}:	Short Circuit Current (Red Response) at Wavelength Above .6um
I_{SCB}:	Short Circuit Current (Blue Response) at Wavelength Below .6um
CFF:	Curve Fill Factor
η:	Solar Cell Conversion Efficiency
L:	Minority Carrier Diffusion Length (D.L.)
I_{MAX}:	Current at Maximum Power Point
V_{MAX}:	Voltage at Maximum Power Point
BSF:	Back Surface Field
BSR:	Back Surface Reflector
V_B:	Bias Voltage
I_o:	Diode Saturation Current
HEM:	Heat Exchanger Method
EFG:	Edge Defined Film-Fed Growth
SOC:	Silicon on Ceramic
RTR:	Ribbon-to-Ribbon
UCP:	Ubiquitous Crystallization Process
SPV:	Surface Photovoltage
MLAR:	Multi-Layer Anti-Reflective
R_s:	Series Resistance